3
Environmental Tracers

3.1 Introduction

In this chapter, the fundamentals of applying environmental tracers will be introduced. The focus will be on applications for the characterization of hydrological systems. While qualitative interpretation will be introduced, quantitative environmental tracer hydrology will be described wherever possible. The useful combination of environmental and artificial tracer applications will be highlighted.

The most common environmental tracers are the isotopes of water $^{18}O/^{16}O$, $^{2}H/H$ and the isotopic ratios of dissolved constituents of water such as the $^{13}C/^{12}C$ ratio of dissolved inorganic carbon or $^{15}N/^{14}N$ of dissolved nitrate. With advances in mass spectrometry and with the advent of new measurement techniques (Inductively Coupled Plasma Mass Spectrometry, ICP-MS, Tunable Diode Laser Spectrography, TDLAS) environmental isotope methods move towards smaller sample amounts and the compound specific analysis of isotopes.

In the context of tracer hydrology, we define environmental tracers as the properties or constituents of water that have not been induced as a result of an intended experiment and which provide qualitative or quantitative information about the hydrological system. Part of environmental tracers that are being used in tracer hydrology result from anthropogenic releases to the atmosphere or to the hydrological cycle: ^{85}Krypton, CFCs and SF_6 have been released into the atmosphere as a result of technical processes – not for the purpose of providing age dating methods for hydrologists. However, these environmental tracers – although environmental concerns or ethical principles might lead us to consider their restriction – have been used and can still be used for hydrological tracer studies, age dating or origin assignment. SF_6, as will be shown, can also be used for artificial trace experiments, when the injection is intended in relation to a defined experiment. A series of pollution tracers, nitrate, organic pollutants, or remnants of past mining activities, can provide information about hydrologic processes. Besides anthropogenic environmental tracers, there are many natural environmental tracers. These include not only stable and radioactive natural isotopes but also chemical compounds such as noble gases and trace elements associated with specific geologic units or lithologies.

Tracers in Hydrology Christian Leibundgut, Piotr Maloszewski, and Christoph Külls

The application of environmental tracers provides methods for the investigation of some major components of hydrological systems: environmental tracers have been used in studies on precipitation processes and origin assignment, open water evaporation, transpiration and stem flow, soil water dynamics, groundwater recharge, subsurface flow mechanisms, runoff components and groundwater studies. The major applications of environmental tracers are:

- *origin assignment of water and water constituents*: more specifically the assignment of recharge altitude or the discrimination of summer or winter recharge, detection of origin of nitrate or dissolved inorganic carbon;
- *hydrological process studies*: identification of runoff components, subsurface flow mechanisms, direct or indirect recharge mechanisms;
- *quantitative determination of flow components*: estimation of evaporation from open water surface, hydrograph separation;
- *determination of residence times*: age dating or analysis of the amplitude of the variation of stable isotopes of water.

The application of environmental tracers is limited by the availability of analytical techniques, knowledge and capacity on tracer methods and resources such as total cost of analysis, total effort of taking samples or time for analysis. The relevance of additional, independent and unique information that can be gained from the application of environmental tracers in relation to the uncertainty associated with these methods defines whether or not environmental isotopes will be useful. Uncertainty in perceptual and conceptual models of hydrological processes and uncertainty in hydrological modelling, especially in the field of subsurface flow processes, constitute fields of hydrological research where environmental tracers provide such unique and relevant additional information.

A major advantage of environmental isotopes is that the input function or the 'injection of tracer' into the hydrological system is provided by nature. Therefore, environmental isotopes can be used on different scales for local, regional and even global studies. If past input functions can be reproduced or reconstructed from data or known physical principles, environmental tracers can also be used for paleostudies or long time scales, for example for the analysis of rainfall origin or recharge in the Holocene or for groundwater flow in drylands. Another key characteristic of environmental isotopes is that they integrate over spatial and temporal scales. A sample taken for the analysis of environmental tracers represents a mixture of flow components characterized by different boundary and flow conditions. This requires another perspective and different methods of interpretation as compared to artificial tracers. The integration of boundary and flow conditions yields complementary information for artificial tracer experiments where only one (or few) points or injection areas in space are marked at one (or few) moments in time.

Therefore, the combination of environmental and artificial tracers can improve the success rate of tracer applications in hydrology significantly. Environmental tracers can be used in the initial phase of planning an artificial tracer test. Residence times and preliminary analyses of flow components may help significantly in reducing failures of artificial tracer tests. They can be used during an artificial tracer test as an additional method. Finally, environmental tracers can be used *a priori* as a backup strategy in the case of a negative tracer test when no breakthrough is received.

3.2 Stable isotopes of water

The most common stable isotopes used in hydrological studies are the stable and radioactive isotopes of water. As pointed out by Gat and Gonfiantini (1981) the fact that oxygen was used as unit mass for chemical weight until 1961 turned the early discovery of oxygen isotopes and of their variability in natural materials (Giauque and Johnston, 1929) into a metrist's nightmare. The resulting efforts in determining the abundance of oxygen isotopes in geological material and especially in water revealed most of the common isotope phenomena being used in modern isotope hydrology. The development and improvement of mass spectrometry techniques, especially the development of the double inlet spectrometer by McKinney *et al.* (1950) and Nier (1957) provided the analytical tools for the description of the variability of isotopes in the water cycle.

3.2.1 Notation

A substance containing the less abundant isotope species N_i and the more abundant isotope N has an isotopic abundance ratio R that is defined by:

$$R = \frac{N_i}{N} \tag{3.1}$$

For natural oxygen and hydrogen compounds N is much larger than N_i. The isotope species can also be expressed in terms of mole fractions $m = N/(N + N_i)$ and $m_i = N_i/(N + N_i)$. The standard mean ocean water (short SMOW) that has been defined by the International Atomic Energy Agency (IAEA) in Vienna as a common standard for expressing isotope ratios (the so-called Vienna SMOW or V-SMOW) has isotopic abundance ratios of (Baertschi, 1976; Hageman *et al.*, 1970):

$$\begin{aligned} R_{^{18}O/^{16}O} &= \left(\frac{^{18}O}{^{16}O}\right)_{VSMOW} = 2005.2 \pm 0.45^{*}10^{-6} \\ R_{D/H} &= \left(\frac{^{2}H}{^{1}H}\right)_{VSMOW} = 155.76 \pm 0.05^{*}10^{-6} \end{aligned} \tag{3.2}$$

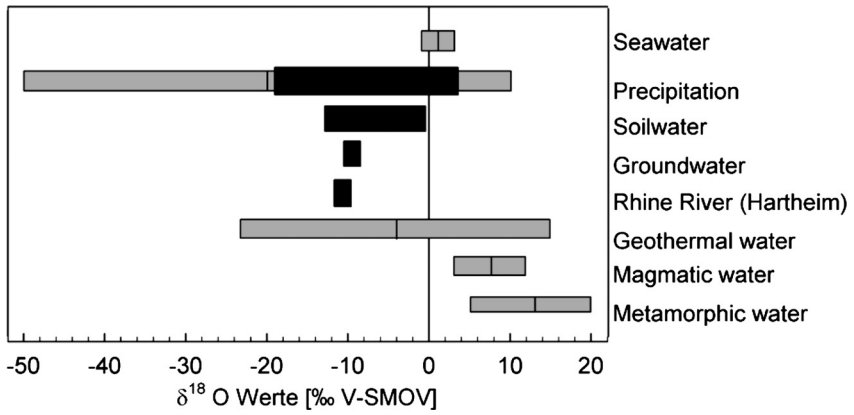

Figure 3.1 Range of isotopes in the water cycle (Königer, 2003 based on Clark and Fritz, 1997). Most common values are marked as black bars.

In general, the isotopic abundance ratio of a sample R_{sample} is given with respect to the internationally accepted standard V-SMOW with the isotopic abundance ratio $R_{standard}$.

$$\delta = \frac{R_{sample} - R_{standard}}{R_{standard}} \tag{3.3}$$

For water samples and many environmental isotopes it is convenient and common to multiply the $\delta^{18}O$ or δ^{2}H values by a factor of 1000 as ‰ difference from the standard being used. In δ notation, positive values indicate an enrichment of ^{18}O or ^{2}H compared to the standard being used whereas negative values signify a depletion of heavier isotopes in the sample. By definition, the ocean has a $\delta^{18}O$ value of $\approx$0‰. The $\delta^{18}O$ of water in the hydrologic cycle ranges from about -50 and -25‰ in ice samples from cold, arctic regions to $+10$‰ in desiccating water bodies and terminal lakes in arid regions (Figure 3.1).

The precision of stable isotope measurements depends on the analytical technique, sampling and sample preparation. For $\delta^{18}O$ determined with double inlet mass spectrometry the error corresponds to about $\pm$0.1‰, for deuterium $\pm$1.0 to 1.5‰. The uncertainty is an important limit for the application of isotope techniques, which needs to be considered in mixing calculations and in origin assignments based on environmental isotopes. Tunable diode laser spectroscopy, an emerging technique for the measurement of stable isotopes, has a precision of about 0.3‰ for $\delta^{18}O$ and of about 1.0‰ for deuterium.

In order to express differences between isotopic ratios in δ notation simply, regardless of a genetic or thermodynamic link, the isotopic difference $\Delta_{A\leftrightarrow B}$ is also used, defined as $\Delta_{A\leftrightarrow B} = \delta_A - \delta_B$

3.2.2 Fractionation

The isotopic composition changes due to fractionation processes. Fractionation occurs if – as a result of a physical or chemical process – the isotopic abundance ratio changes. Phase changes, evaporation, condensation, freezing, sublimation, melting and some chemical reactions are associated with an isotopic fractionation. In order to describe fractionation, a fractionation factor α is used, that is defined by:

$$\frac{dR}{R} = \left(\frac{dN_i}{dN}\right) \Big/ \left(\frac{N_i}{N}\right) = \alpha \tag{3.4}$$

According to a model suggested by Urey (1947), equilibrium fractionation arises from the exchange of isotopes between different phases (i.e. water and vapour) or chemical species at equilibrium conditions. For a specific reaction at full equilibrium, the degree of fractionation is then expressed by:

$$\alpha_{A \leftrightarrow B} = \frac{R_A}{R_B} \tag{3.5}$$

where R_A and R_B represent the isotopic ratios of the two phases A (*water*) and B (*vapour*). In ‰ notation also the enrichment factor $\varepsilon_{A \leftrightarrow B}$ is used. The enrichment factor is defined as:

$$\varepsilon_{A \leftrightarrow B} = \left(\frac{R_A}{R_B} - 1\right) {}^{*}1000 = (\alpha_{A \leftrightarrow B} - 1) {}^{*}1000 \tag{3.6}$$

The approximate relation between the enrichment factor $\varepsilon_{A \leftrightarrow B}$ and the fractionation factor $\alpha_{A \leftrightarrow B}$ in the form $\varepsilon_{A \leftrightarrow B} \approx 10^3 \ln \alpha_{A \leftrightarrow B}$ only holds for small enrichment factors, because of the approximation $\ln \alpha \approx 1 - \alpha$ when $\alpha \approx 1$.

For the stable isotopes of water, ice $\leftrightarrow$ water $\leftrightarrow$ vapour phase transitions are of special importance. Fractionation between different phases of water results from differences in the physical properties of water molecules containing different isotopic species of oxygen and hydrogen. As an example, the water vapour pressures of the species $^1H_2{}^{16}O$ and $^1H_2{}^{18}O$ differ by about 1% at 20 °C (Szapiro and Steckel, 1967, Figure 3.2). This difference in physical properties causes a higher diffusion of $^1H_2{}^{16}O$ into the ambient air as compared to $^1H_2{}^{18}O$ during the evaporation process. Hence, there results a depletion of the heavier molecules of $^1H_2{}^{18}O$ in the gaseous phase.

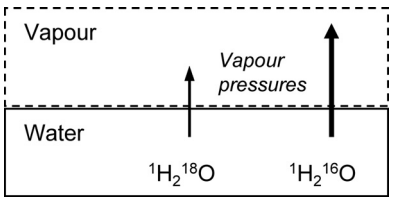

Figure 3.2 Differences in the vapour pressure for the two isotope species $^1H_2{}^{18}O$ and $H_2{}^{16}O$ during equilibrium exchange with water vapour.

For ^{18}O a fractionation factor of $\alpha^{18}O_{water\leftrightarrow vapour} = 1.0093$ was measured for equilibrium phase transitions between water and vapour at 25 °C. The fractionation factor for ^{2}H during the same equilibrium phase transition is as high as $\alpha^{2}H_{water\leftrightarrow vapour} = 1.076$ (Majoube, 1971).

Isotope equilibrium fractionation is also a function of temperature. Szapiro and Steckel (1967) and Majoube (1971) found that the fractionation factor $\alpha_{A\leftrightarrow B}$ generally follows an equation of the type:

$$10^{3*} \ln \alpha_{A\leftrightarrow B} = 10^{6} a/T^{2} + 10^{3} b/T + c \tag{3.7}$$

where T is the ambient water temperature in K and a, b, c are coefficients. Tabulated values for a, b and c for the most common thermodynamic reactions in hydrogeological systems are given in Clark and Fritz (1997). They also give data on their homepage at www.science.uottawa.ca/eih. More than 1100 fractionation equations are described at the site of the Department of Geology of the University Laval/Quebec in Canada (http://www.ggl.ulaval.ca/cgi-bin/isotope/generisotope.cgi).

For water ↔ vapour equilibrium exchange, the fractionation is higher at low than at high temperatures. The equilibrium fractionation as a function of temperature is shown in Figure 3.3. This dependence is the dominant process in many hydrological systems and contributes – together with other processes – to a series of macroscale effects described below such as the latitude effect, the altitude effect, the continental effect, the amount effect and the seasonal effect.

Often, the assumption of isotopic equilibrium is not met and so-called kinetic fractionation processes take place. This may be caused by rapid temperature changes or the removal or addition of the product or reactant during the reaction. Major nonequilibrium processes in hydrological systems are *'diffusive fractionation'* and *'Rayleigh distillation'*.

Diffusive fractionation is the fractionation of isotopes caused by diffusion processes. In hydrological systems diffusive fractionation occurs, for example during the

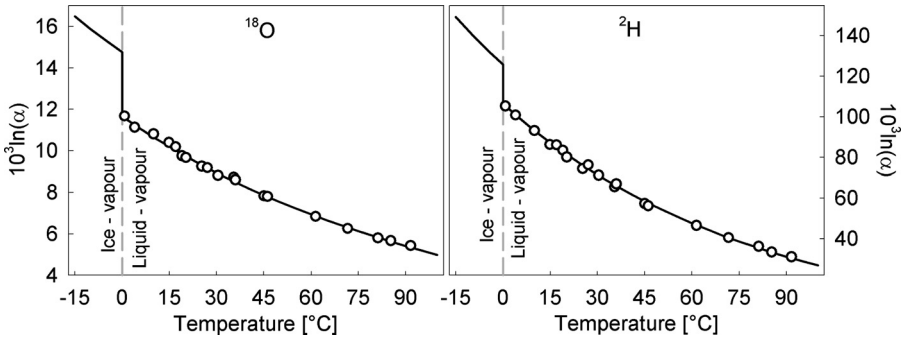

Figure 3.3 Temperature dependence of equilibrium fractionation, at °C the equilibrium is established for the ice-water phase assemblage (dashed line), causing a step in the temperature-equilibrium function (data are from Majoube, 1971).

evaporation process when water vapour diffuses into air. Diffusive fractionation results from the different molecular velocities of different isotopes. The molecular velocity depends on temperature (usually given in Kelvin) and on the mass of the atom or molecule according to statistical particle mechanics:

$$v = \sqrt{k * T / (2 * \pi * m)} \ [\mathrm{m/s}] \tag{3.8}$$

with the Boltzmann constant $k = 1.3806504 \cdot 10^{-23}$ J/K, the absolute temperature T in Kelvin, and the molar mass m in kg. As the unit of Joule corresponds to [kg*m^2*1/s^2] with m = metres and s = seconds in SI units the resulting unit is [m/s]. From this equation, the diffusion of two isotopes of different masses in vacuum can be derived. From the molecular velocity of isotopes it can be shown that the diffusion rates for an ideal gas in a *vacuum* are just inversely proportional to the square root of the mass of its particles – the other constants and also temperature (!) cancel out:

$$\alpha_{diffusion\ (A-B)} = \sqrt{\frac{m_B}{m_A}} \tag{3.9}$$

where m_A and m_B are the respective molecular weights of different substances. If this principle, known as Graham's law of effusion, is applied to dry air, the molecular mass of dry air needs to be taken into account. The molecular mass of dry air can be derived from the average gas composition and the molecular weights of its constituents and corresponds to about 28.8 (see also Clark and Fritz, 1997):

$$\alpha_{diffusion\ air\ (A-B)} = \sqrt{\frac{m_B * (m_A + 28.8)}{m_A * (m_B + 28.8)}} \tag{3.10}$$

The resulting fractionation factors can be derived and transformed into an isotope difference using Eq. (3.6). The kinetic effect by diffusion $\varepsilon_{A \leftrightarrow B} = (\alpha_{A \leftrightarrow B} - 1)$ is 32.3‰ for $H_2{}^{18}O/H_2{}^{16}O$ and 16.6‰ for $^2H_2O/^1H_2O$. Hence, the fractionation by diffusion is stronger for oxygen isotopes than for deuterium isotopes. The above equation holds for dry air with a humidity of 0% only.

As we deal with real hydrological systems we need to include the effect of atmospheric humidity and turbulence. In a series of laboratory and field experiments the process of evaporation from an open water surface into an atmosphere with a relative humidity h in % has been studied. Gat (1970) Merlivat (1978) and Vogt (1976) report empirical values between 13 and 28.5‰ for $H_2{}^{18}O/H_2{}^{16}O$. In general isotopic differences resulting from kinetic fractionation in natural and turbulent systems are much smaller compared to diffusive fractionation only. Empirical values reported by Gonfiantini (1986) are commonly used stating that the kinetic fractionation factor given in ‰ is in proportion to $(1 - h)$ with h = humidity in %:

$$\begin{aligned} \Delta\varepsilon_{18O} &= 14.2 * (1 - h)[‰] \\ \Delta\varepsilon_{2H} &= 12.5 * (1 - h)[‰] \end{aligned} \tag{3.11}$$

For deuterium also the theoretical approach yields a kinetic fractionation that is higher than for diffusion (16.6 to 12.5‰). Apparently for real and turbulent systems the ratio of diffusion coefficients scales to $(D_A/D_B)^n$ with a turbulence parameter n for which $0 \geq n \leq 1$. Many experimental data fit with n = 0.5 that is the square-root of the diffusion coefficients $\sqrt{D_A/D_B}$.

As evaporation in real hydrologic systems differs from a pure diffusion process, it makes sense to define a kinetic fractionation by turbulent diffusion. While a water-vapour assemblage in a closed system would simply equilibrate according to Equation (3.11), in open systems there is an additional kinetic fractionation. For this process, resistance is in inverse proportion to the diffusion coefficients D_A and D_B or $\pi_i \sim 1/D_i$. Based on the concept of resistance controlling the flux of isotopes, it is stated that:

$$\varepsilon_{kinetic\ (water\ -\ vapour)} = (1-h)^* \left(\frac{\rho_i}{\rho} - 1\right) \tag{3.12}$$

It follows that the slope of an evaporation line depends on the humidity during evaporation. At high humidity (>85%) the slope is steeper approaching that of the meteoric water line and at low humidity the slope is dropping. In arid regions slopes of less the five can be observed.

The processes above are simplified and idealized representations of processes occurring in nature. Craig, Gordon and Horibe (1963) introduced the concept that evaporation results from a combination of several interconnected processes as summarized in Figure 3.4.

They propose that above an open water surface equilibrium fractionation takes place in a thin liquid-vapour interface layer that is vapour-saturated. The isotopic composition in this interface layer depends initially on temperature dependent equilibrium fractionation and on the initial isotopic composition of the liquid phase. In a second step vapour diffuses from this saturated interface layer. This process can be approximated by molecular diffusion, as described above. The diffusion process depends on the humidity in the diffusion layer and on the mass ratio of isotopes. The vapour finally enters the turbulent mixing zone of the atmospheric boundary layer and is mixed with the advected vapour of a given isotopic composition. In the turbulent boundary layer

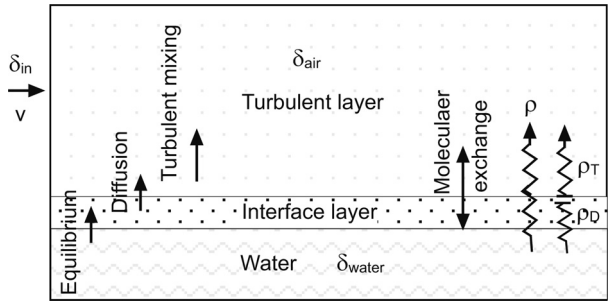

Figure 3.4 The concept of water-atmosphere exchange as a process in four steps: equilibrium-diffusion-mixing and re-equilibration.

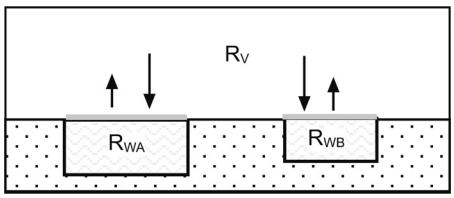

Figure 3.5 The exchange of isotope concentrations between two reservoirs by gas diffusion in a closed system.

no fractionation is assumed to take place. The mixed vapour then partially re-enters the diffusion layer and may re-precipitate at the surface of the liquid layer causing a molecular exchange. This equilibration may even result in an isotopic exchange between two fluid reservoirs that are connected with a common atmosphere in a closed system (Ingraham and Criss, 1993, Figure 3.5).

The advantage of this concept is that it allows a step-wise description of processes – the disadvantage is that the resulting integration of these processes is becoming quite complex:

$$\begin{aligned} E &= (c_{liquid} - c_{air})^* \frac{1}{\rho} \quad with \quad h = \frac{c_{air}}{c_{liquid}} \quad relative\ humidity\ in\ [\%] \\ E &= (c_{liquid} - h^* c_{liquid})^* \frac{1}{\rho} = c_{liquid}{}^* (1-h)^* \frac{1}{\rho} \end{aligned} \tag{3.13}$$

where E is evaporation, h is the relative humdity and c_{liquid} the absolute moisture or vapour pressure above the open water surface, c_{air} the absolute moisture or vapour pressure in the atmospheric boundary layer and ρ the resistance coefficient for the flux of moisture. This equation is similar to turbulent diffusion equations widely used in meteorology for boundary layer physics. At this stage the isotopic ratios R, R_{liquid} and R_{air} can be introduced:

$$E = c_{liquid}{}^* \left(\frac{R}{\alpha} - h^* R_{air} \right)^* \frac{1}{\rho_i} \tag{3.14}$$

with ρ_i the specific resistant coefficient for an isotope. Gonfiantini (1986) discusses different aspects of this equation, notably the case in which the isotopic composition in the water column is not homogeneous. In a stratified lake c_{liquid} corresponds to the epilimnion. In the case of the uppermost part of the water column the isotopic composition is different. An additional resistance term needs to be specified because of incomplete mixing – however, in general this is not considered necessary.

Another important kinetic fractionation process is the Rayleigh distillation. It can be used to describe systems where the reactant is continuously being removed by, for example, rain-out from clouds or evaporation. The distillation equation states that the isotopic ratio R is a function of the initial ratio R_o, the fraction of water remaining in the reservoir f and the fractionation factor:

$$R = R_o f^{(\alpha - 1)} \tag{3.15}$$

For Rayleigh distillation processes, the fractionation increases strongly when the residual water fraction approaches small values. The Rayleigh formula was developed for distillation processes. It is obtained from the differential equation relating the fractionation factor to the mass change. However, it is only valid if the fractionation factor is constant or can be approximated by a constant value. For condensation processes that cause altitude effects, the differential equation should be used and integrated with a variable temperature.

3.2.3 The global distribution in rainfall

A review of time series from a global survey of stable isotopes in rainfall (Rozanski, Araguás-Araguás and Gonfiantini, 1993) reveals patterns in their seasonal and geographic distribution. These patterns are the result of the fractionation processes described above that take place in the hydrologic cycle. The so called '*isotope effects*' are the basis for the interpretation of isotope data in hydrogeological studies. Craig (1961) found that, at a global scale, δ^{18}O and δ^{2}H in surface waters are characterized by the correlation $\delta^2 H = 8\delta^{18} O + 10‰$ (this equation was established for the SMOW reference, Standard Mean Ocean Water). The equation defines the *global meteoric water line*. The isotopic composition of precipitation in humid regions corresponds to this relationship for most continental stations (Figure 3.6).

At a regional scale deviations from this global correlation exist and specific regional meteoric water lines have been introduced, for example for the Mediterranean or some coastal regions. Meanwhile, a slightly modified relationship based on the data of the IAEA global network of isotopes in precipitation (GNIP) has been proposed by Rozanski, Araguás-Araguás and Gonfiantini (1993). This revised regression has a slope of $8.17 \pm 0.07‰$ and an intercept of $11.27 \pm 0.65‰$. It takes into account rainfall data from the IAEA only and is based on the *VSMOW* standard. In some cases, it is necessary to use other regional meteoric water lines or to define a local meteoric water line. However, this should be done only based on a regional analysis as local meteoric

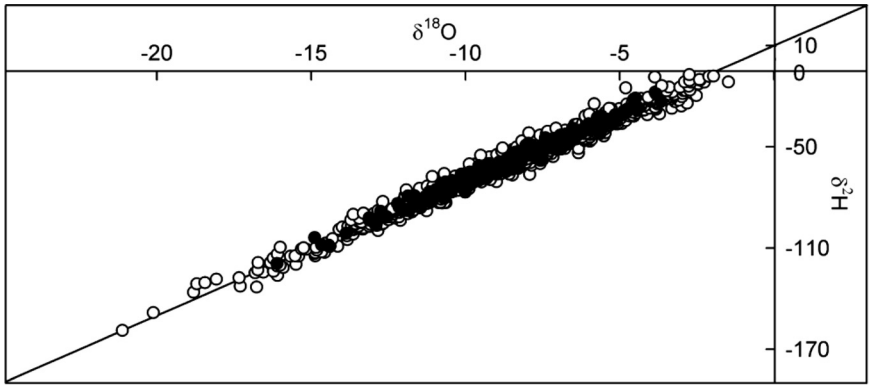

Figure 3.6 Isotopes in rainfall as such (open circles) and weighted with rainfall amount (full circles) for the Dreisam catchment, Germany (1998–2008).

water lines might be influenced by deficiencies of the sampling network or procedures and be therefore more misleading than an advantage. Especially in islands, coastal areas or tropical mountain areas, rainfall might deviate from the global meteoric water line.

3.2.3.1 Temperature effect

Fractionation factors depend on temperature. During water ↔ vapour phase transitions fractionation is more pronounced at low temperatures. As a result, the isotopic composition of rainfall in cold environments is more depleted compared to warm environments.

In Figure 3.7 the dependence between mean $\delta\ ^{18}O$ values and mean annual temperature has been plotted for different regions. These dependencies exist for ^{18}O and for ^{2}H. Combining both, a general thermometer can be developed. The stable isotope thermometer reflects the ambient temperature of different sites (see the examples of Alaska, Switzerland, Greece, Namibia and Argentina). It can be used directly to estimate the temperature from stable isotope values. Dansgaard (1964) derived temperature effects of precipitation based on a theoretical treatment of cooling processes

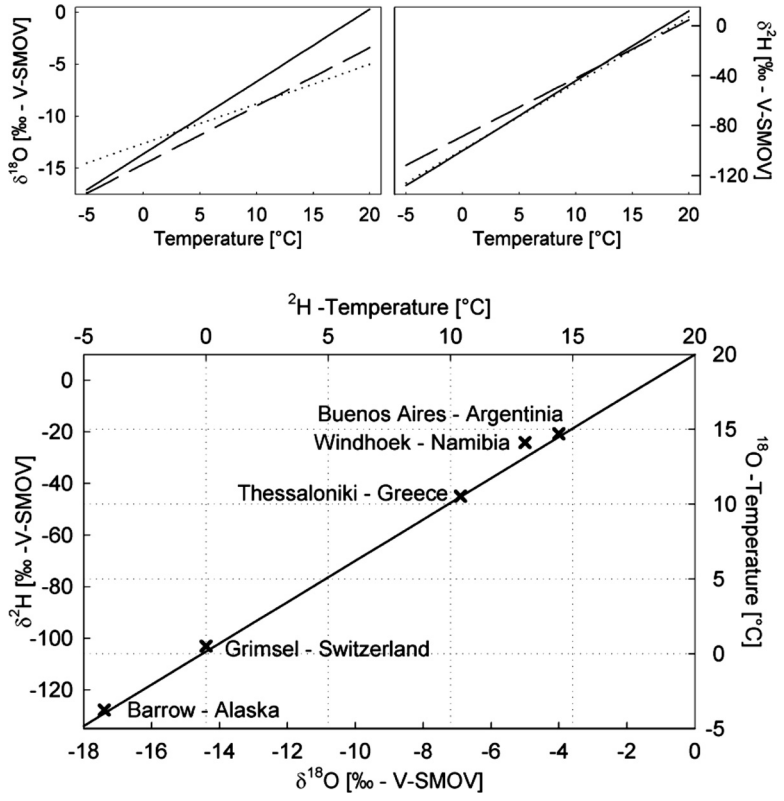

Figure 3.7 Upper graph: different observed regional temperature effects. Lower graph: The influence of mean annual temperature on the isotopic composition of ^{18}O and ^{2}H, Dansgaard (1961, 2004). Crosses mark values at −5, 0, 10 and 15 °C mean annual temperature.

at different boundary conditions (isobaric, isothermal). Based on measurements an isotope thermometer of about:

$$\delta^{18}O = -0.69\ t_a - 13.6\,‰ \tag{3.16}$$

is given, where t_a is the mean annual air temperature in °C. For temperatures below 0 °C the temperature effect increases to about 0.95‰/°C at −20 °C. A major part of the temperature effect can be derived from the dependence of the fractionation factor on temperature and from the fractional distillation of water by cooling processes.

3.2.3.2 Seasonal effect

Often a seasonal fluctuation of stable isotope ratios is observed as a result of temperature effects, different trajectories of air masses and varying fractionation processes in the source area of atmospheric moisture.

The seasonal effect can be used and is important for input functions to the hydrological system. In general, the seasonal isotope effect of continental stations closely follows the temperature regime. In coastal areas, the seasonal effect is less pronounced. This is shown in Figure 3.8 (top) for the station Cuxhaven. Based on known principles of

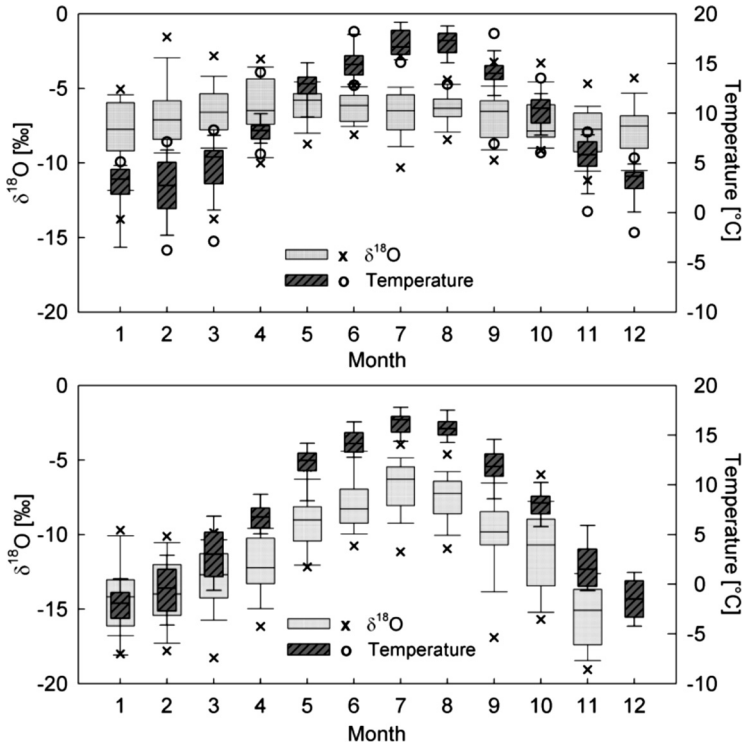

Figure 3.8 Seasonal effect – data isotopes in rainfall of Germany (Cuxhaven (above) – Garmisch (below): 1978–2002; Temperature in °C: 1984–2002).

fractionation and a conceptual model of the hydrological cycle there are several factors producing a seasonal effect:

- the temperature in the source region of atmospheric moisture will change the fractionation during evaporation,
- circulation of air masses and transport processes will cause advection of moisture from different origins and modify the original isotopic composition of moisture,
- and finally, the conditions during rainout (ambient temperature, absolute moisture and phases (snow, rain) will change.

If the seasonal variation of isotopes in precipitation is known, observations at different soil depths, in runoff and in groundwater time series can reveal the travel time and mean residence time of the system (see below).

3.2.3.3 Altitude effect

In general, precipitation is depleted increasingly at higher altitude. This is the combined result of temperature effect and moisture depletion by adiabatic cooling. Equilibrium fractionation increases with lower temperatures, making fractionation more efficient at higher altitudes. Repeated rainout during uplift of air masses causes a Rayleigh-type distillation process.

Altitude effects are often given only for annual mean rainfall. It also exists within different seasons (see Figure 3.9). The example of Cyprus shows that the variability of

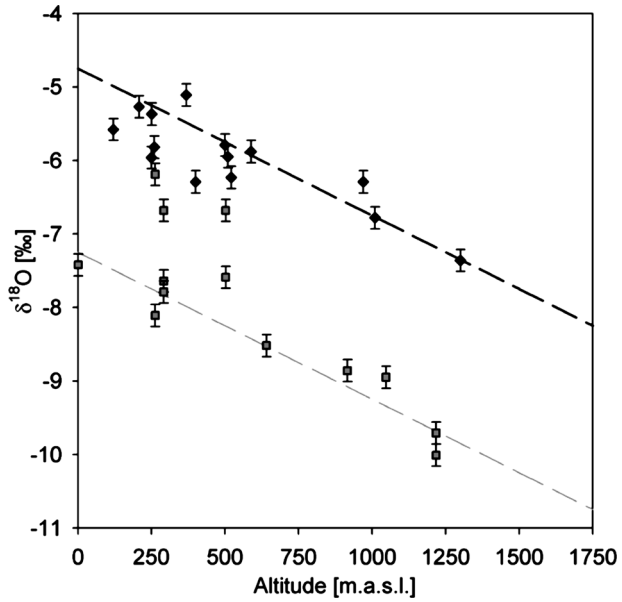

Figure 3.9 Altitude effect of winter (grey) and summer (black) precipitation (data from Cyprus).

rainfall is higher close to the coast, with increasing distance from the coast and therefore increasing altitude specific altitude effects develop in summer and in winter time.

A number of observed altitude effects exist. For $\delta\,^{18}O$ the range of observed altitude effects is between $-0.1‰$ and $-0.36‰$/ 100 m. Dansgard (1964) presents a theoretical calculation of altitude effects and demonstrated that the altitude effect can be derived from the adiabatic cooling rate of air temperature in a straightforward way: the theoretical gradient is about $-0.36‰$ 100 m for $\delta\,^{18}O$. As Gat, Mook and Meijer (2000) point out, the altitude effect differs from the latitudinal effect because the decreasing pressure requires a higher temperature decrease to reach saturated water vapour pressure. As a result the change in moisture per change in temperature (°C) is smaller than for isobaric condensation.

In some cases other factors also affect the composition of precipitation at different altitudes: different precipitation generation processes or mixing of air masses with different trajectories. Therefore, altitude effects need to be verified in each region in order to take into account these additional effects.

In remote areas especially the altitude effect is a key to hydrological studies. Recharge altitude, origin of water and conceptual models can be validated based on known altitude effects. The problem is that often data on local altitude effects are not available. Data from the IAEA GNIP network can be retrieved and used for a regional analysis with similar atmospheric circulation patterns. However, in many parts of the world, the network is not dense enough. Experimental isotope networks can be set up to provide such data. But these require at least a few years of measurement campaigns. There are two principle approaches to overcoming such problems. In principle, the altitude effect can be derived from a physical model of condensation and rainfall generation.

If the physics of water condensation and fractionation are taken into account, the relationship above between adiabatic cooling rate and isotopic composition can be derived. The adiabatic cooling rate can be retrieved from climatological network data. However, this estimate may be biased by specific local conditions and should be verified by an experimental approach.

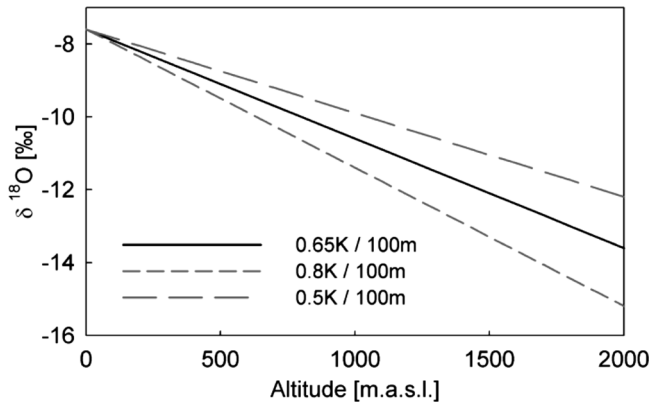

Figure 3.10 Altitude effect for different adiabatic cooling gradients.

A field method for verifying altitude effects consists of sampling shallow groundwater from very small watersheds with sufficiently long mean residence times to provide an average value of mean annual rainfall (>2 years) and sufficiently short flow distance from the recharge area to represent the conditions at the altitude of sampling. This practical approach uses the hydrological system as a natural integrator of rainfall samples. Based on a terrain analysis small catchments can be selected that represent an altitude range. Close to the watershed groundwater can be sampled from springs or shallow groundwater boreholes. These samples can be used to reconstruct the altitude effect. This altitude effect does not correspond to the weighted rainfall – it represents the weighted groundwater recharge. This, however, can be exactly what is needed for an origin assignment of groundwater recharge. Vogel, Lerman and Mook (1975) has adopted this approach to characterize the altitude effect of the Andes mountains. Together with modern GIS techniques this approach can be used to preselect sampling locations based on terrain analysis and an available borehole database.

It is interesting to note that the altitude effect and the analytic precision determine the accuracy of any determination of recharge altitude. In general, we assume $\pm 0.1‰$ for $\delta\,^{18}O$ and $\pm 1.0‰$ for $\delta\,^{2}H$. Therefore it is unrealistic to resolve the recharge altitude within less than the isotope altitude gradient divided by at least two times the analytical precision. Best results are obtained in mountain areas with distinct differences in recharge altitude well exceeding this uncertainty.

3.2.3.4 Continental effect

For large trajectories of air masses precipitation becomes more depleted with increasing distance from the coast. Since the vapour is mainly derived from oceans, water in clouds will become depleted in heavier isotopes with each rainfall event along the trajectory. This phenomenon is termed continental effect. Continental effects are relevant for characterizing the isotopic composition at continental or global scale.

The continental effect is caused by the gradual depletion of air masses by precipitation as they cross continents or move towards the interior of continents. Each condensation and precipitation event at a given temperature causes a fractionation. The accumulation of these effects leads finally to an isotopic depletion of air masses as they move from their source areas. This effect is reduced by transpiration and re-evaporation on the continent. As such the process can be modelled and quantified. Holtkamp (2008) developed a hydrological model of continental isotope effects:

$$R = R_o\, f^{(\alpha-1)} \quad with \quad f = \frac{Q_a - \int(P(\tau)dt + \int E(\tau)\ dt}{Q_a} \tag{3.17}$$

with R and R_o isotope ratios, f remaining fraction of water and α a temperature dependent fractionation factor. The fraction f is derived from a hydrological balance involving the inflow of moisture from the ocean Q_a and the hydrological balance $P(\tau) - E(\tau)$ that are here given as a function of trajectory length t.

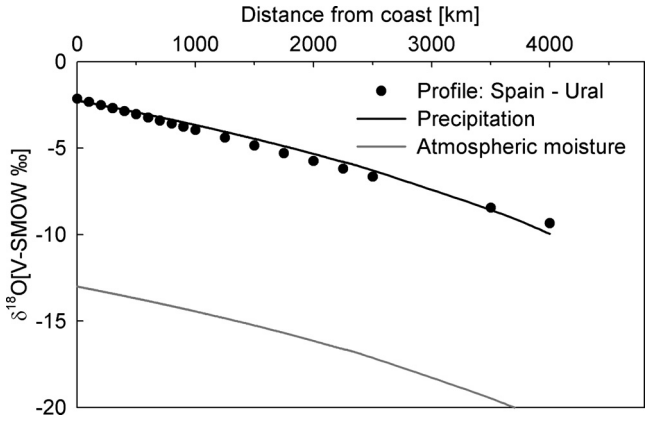

Figure 3.11 Continental effect for Europe modelled with a hydrological Rayleigh process.

The hydrological model of continental effects can be used to describe continental effects based on rainfall, evaporation (rainfall recycling), wind speed and moisture content (determining Q_a). It can be shown that the continental effect increases with rainfall amount and decreases with recycling of air masses by evaporation. Increased moisture flux (higher wind speed, absolute moisture) will reduce continental effects. Continental effects can be modelled as a result of these factors for different climatic conditions.

Different attempts have been made to integrate all atmospheric isotope effects into a general model. Dansgaard (1964) developed a conceptual model for isotopes in precipitation based on the assumption that the vapour mass moves from the oceanic origin to the condensation site without further mixing. Thus the isotopic composition of vapour and rain depends mainly on equilibrium fractionation and the fraction of vapour lost by the rainout process due to the temperature gradient between the source region and the precipitation site. This can be modelled by the Rayleigh distillation equation, which has been improved by incorporating the kinetic fractionation during evaporation from the ocean (Merlivat and Jouzel, 1979) or during the formation of ice crystals (Jouzel and Merlivat, 1984). Although these models predict high-latitude isotope – temperature dependence realistically, they are not able to describe the mixing of different air masses, the influence of evapotranspiration over continental surfaces or convective cloud processes (Sturm *et al.*, 2005).

While the isothermal Rayleigh fractionation formula is often used, adiabativ cooling in fact represents a nonisothermal process. This can be described by applying the differential form:

$$\frac{dR}{dN} = \frac{R}{N}\left(\alpha(T) - 1)\right) \tag{3.18}$$

where R is the isotopic ratio of the stable isotope species, N the total mass and $\alpha(T)$ a temperature dependent fractionation factor. The difference between the integrated

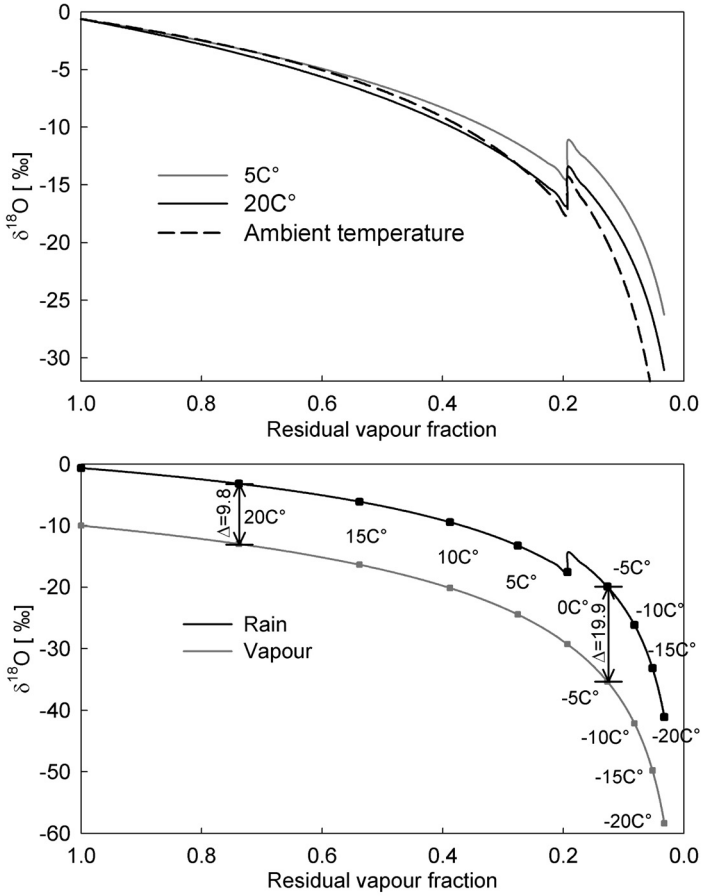

Figure 3.12 Isothermal and nonisothermal Rayleigh fractionation and resulting isotopic composition of vapour and rain.

and the differential equation is shown in Figure 3.12. For higher temperatures and fractions $f \gg 0$, the difference is small. For low temperatures and small fractions the difference increases and becomes relevant.

3.2.3.5 Regionalization of isotopes in rainfall

Regionalization of isotopes in rainfall is being used to define input functions for time and spatial distributions. Regional maps are very useful for origin assignment of water and for macroscale modelling of hydrological response by isotopes. Yurtsever and Gat (1981) found regional relationships between mean isotopic composition of precipitation and geographical and climatological parameters by performing multiple linear regression analyses on the GNIP database. Beginning the regressions with the parameters precipitation, latitude, altitude and temperature and then eliminating them one by

one, they found out that the use of precipitation, latitude and altitude besides temperature did not lead to a considerably better correlation between observed and predicted monthly mean ^{18}O values (for simple and for amount-weighted means). Temperature is the main parameter of importance. In a joint IAEA – University of Waterloo project Birks *et al.* (2002) re-evaluated and reconstructed GNIP station-based data to produce global and regional maps of the amount-weighted annual and monthly mean ^{18}O and ^{2}H values of precipitation. Bowen and Wilkinson (2002) empirically modelled relationships between amount-weighted annual mean ^{18}O values of modern precipitation and latitude and altitude using the third release of the GNIP database (IAEA/WMO, 2006). As the isotopic composition of precipitation is controlled by Rayleigh distillation, which in turn mainly depends on temperature, Bowen and Wilkinson (2002) argue that one has to include the geographic parameters that control temperature, that is latitude and altitude.

Looking at the spatial distribution of the residuals between observed and calculated values Bowen and Wilkinson (2002) concluded that the ^{18}O values of precipitation depend primarily on latitude and altitude dependent temperature variations. An example of regionalization of isotopes in rainfall is given in Figure 3.13 for Germany. The scale represents light (white) and heavy (dark) signature changing with time and in space. The precision of the map is $\pm 0.4‰$.

3.2.3.6 Evaporation

Evaporation from surface water causes an enrichment in the remaining water with a slope that is smaller than the slope of the meteoric water line in the $\delta^{18}O$-$\delta^{2}H$ diagram. Typically, evaporation slopes are between 4 and 5.5.

Fractionation by evaporation from open surface water is obviously a key process in the generation of atmospheric moisture above the oceans. It is also known to characterize the isotopic composition of lakes and of temporary surface depressions (Dody *et al.*, 1995).

For evaporation from open surface water, the slope depends on the atmospheric conditions during evaporation (Gonfiantini, 1986). In general, the slope of values in a $\delta^{18}O$–$\delta^{2}H$ diagram increases with increasing humidity and decreases with lower humidity. Figure 3.14 shows evaporated water samples deviating from the global meteoric water line. While isotope data from different aquifers are often diffuse (above), samples characterized by similar meteorological conditions and stemming from the same source of water provide a characteristic evaporation line (Figure 3.15, below).

A characteristic evaporative enrichment of groundwater below dunes was found in arid and semiarid climate (Dinçer, al-Mugrin and Zimmermann, 1974; Allison, Stone and Hughes, 1985). The observed enrichment, with a small slope of about two in a $\delta^{18}O$–$\delta^{2}H$ diagram, is seen as a result of vapour diffusion from soil moisture prior to recharge. Evaporation can remove moisture from a soil column by diffusion. Diffusive evaporation from a soil column results in a low-slope evaporation line in a $\delta^{18}O$–$\delta^{2}H$ diagram (Dinçer, al-Mugrin and Zimmermann, 1974; Allison, Stone and Hughes, 1985; Gat, 1995).

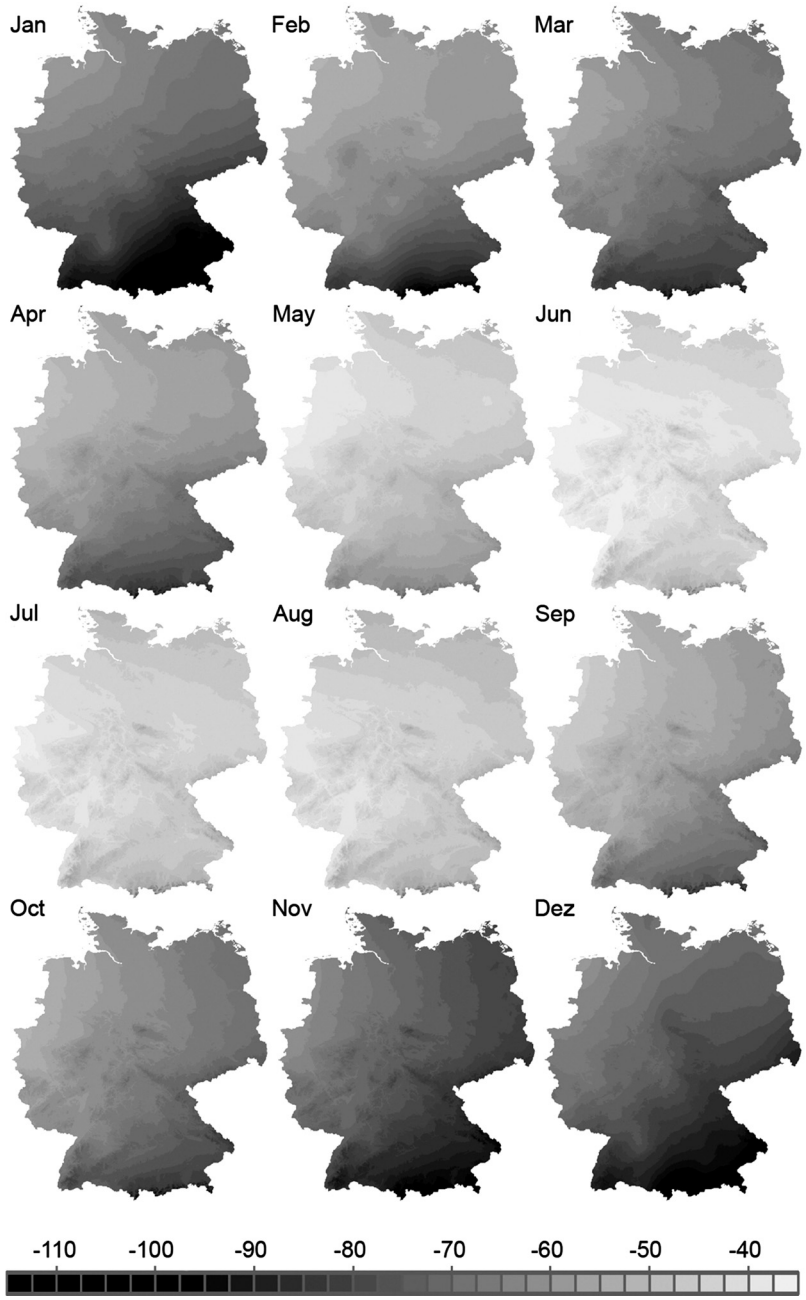

Figure 3.13 Calculated deuterium isotopes (in ‰ δ – V-SMOW) in rainfall for Germany (modified after Schlotter, 2007).

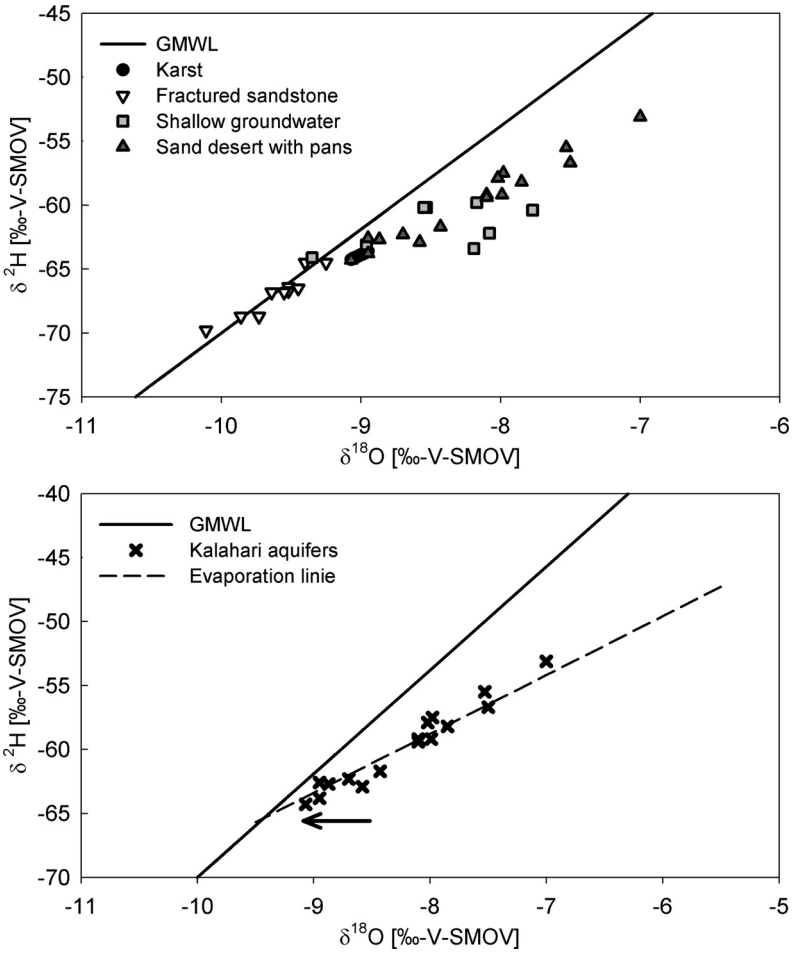

Figure 3.14 $\delta^{18}O$–$\delta^{2}H$ diagrams of groundwater samples from the Kalahari. The continuous line represents the Global Meteoric Water Line, the dashed line the evaporation line fitted by linear regression.

A correction of $\delta^{18}O$ for evaporative enrichment according to Geyh and Ploethner (1997) can be applied. Corrected values indicate the isotopic composition without enrichment by evaporation. As the corrected value marks the intersection of the evaporation line with the Global Meteoric Water Line, it is defined by:

$$\delta^{18}O_{corrected} = \frac{\delta^{2}H_{measured} - e^{*}\delta^{18}O_{measured} - d}{8 - e} \tag{3.19}$$

where e corresponds to the slope of the evaporation line determined, for example, as 4.5, and d is the deuterium excess of global precipitation, with d = +10‰. Once the $\delta^{18}O$ has been corrected for evaporation, the corresponding deuterium value can be obtained by solving the equation for the global meteoric water line. This method is

extremely useful in studying flow paths of surface and groundwater that have been affected by evaporation. Once the evaporation effect has been corrected for, it can be analysed whether the original water type is prevailing or whether mixing with another source of water (resulting in different δ^{18}O values) takes place.

It is important to note that only conditions where (a) kinetic fractionation takes place and where (b) a reservoir is partially depleted result in evaporation effects. If a high number of small depressions are completely evaporated, no isotope effect results. Therefore complete evaporation from interception storage (leaves) leaves hardly any isotope signal. However, if small storages evaporate partially, significant isotope effects result. Detailed sequential sampling of rainstorms in the arid Negev Desert, Israel, revealed strong isotopic variations ($-2‰$ to $-9‰$ δ^{18}O) between different rain spells within hours. Interestingly, a rain spell with low intensity but long duration was more depleted than preceding and following short, intensive spells (Dody *et al.*, 1995; Adar *et al.*, 1998). These data indicate, that partial depletion of surface depressions and subsequent flushing may result in high evaporative enrichment because this a Rayleigh type process.

The evaporation of water from lakes can be estimated from water and isotope mass balances. Water and isotope mass balances have been used based on tritium data (Gat, 1970) and recently for water balances of large river systems (Königer *et al.*, 2008). The water balance of a lake is:

$$\frac{dV}{dt} = Q_{in} + P - Q_{out} - E \tag{3.20}$$

where V is the volume of the lake, Q_{in} and Q_{out} are in- and outflow, P precipitation and E evaporation. The general water and isotope balance approach is given by the equation below. Additional terms can be added for different types of inflow (surface, groundwater). The balance equation writes:

$$\frac{d(V^*\delta_V)}{dt} = {Q_{in}}^*\delta_{Q_{in}} + P^*\delta_P - {Q_{out}}^*\delta_{Q_{out}} - E^*\delta_E \tag{3.21}$$

where δ_i represent the respective isotopic composition of the hydrological component identified by the subscript i. Difficulties arise from the fact, that the lake volume is not fully mixed. The isotopic composition of the lake can be determined by adequate sampling. The isotopic composition of rainfall, inflow and outflow need to be determined in the field. The major difficulty is the determination of δ_E which depends on transport processes through the boundary layer and on atmospheric conditions such as wind speed and relative humidity. Different approaches were presented to use the balance equation for the estimation of evaporation flux and for lake water balances (Gat and Gonfiantini, 1981; Mook, 2001).

For well-mixed steady state systems Gibson *et al.* (1993) proposed an estimation based on a two-component mixing approach according to:

$$\frac{E}{P} = \frac{(\delta_P - \delta_V)}{(\delta_E - \delta_V)} \tag{3.22}$$

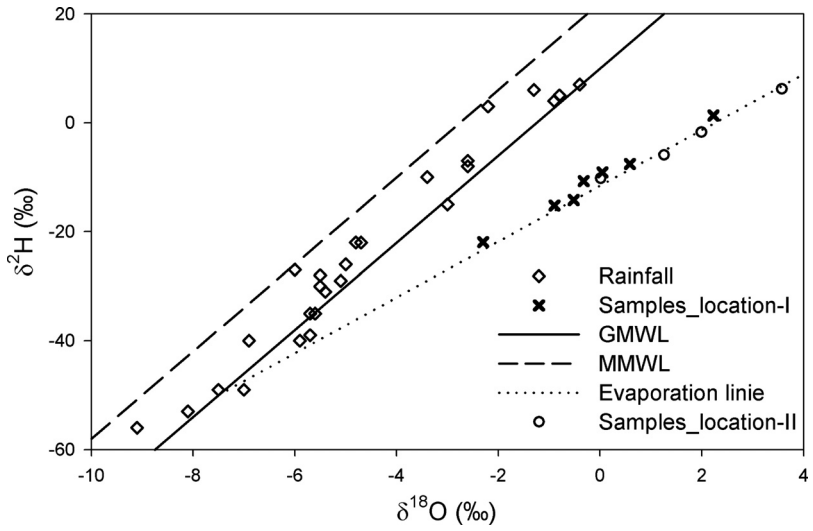

Figure 3.15 Evaporation from open surface water, example from Pantanal wetland/Brazil with local rainfall (squares), and two water bodies with different degrees of evaporation (modified from Schwerdtfeger, 2009).

where the subscripts P, V and E represent the mean weighted local isotopic composition of precipitation, lake water and evaporating moisture. While the isotopic composition of lake water and precipitation can be obtained by sampling, the isotopic composition of evaporating moisture needs to be determined by field experiments, for example with evaporation pan experiments or through calibration for lakes with known water balance or based on theoretical relationships. This approach works only for steady-state systems as long as evaporation does not affect the lake volume significantly.

If evaporation reduces the lake volume, the Rayleigh equation can be applied to estimate the evaporated volume for progressive evaporation in a simplified way based on:

$$\frac{E}{V} = 1 - \exp \frac{(\delta_V - \delta_i)}{\frac{1}{\alpha} - 1} \tag{3.23}$$

where δ_V is the isotopic composition of the well-mixed water body after evaporation E took place, δ_i the initial isotopic composition and α the fractionation factor. This approach only holds for idealized small and well-mixed water bodies (ephemeral pans with depths <1 m) and does not take into account the exchange with atmospheric vapour.

A more accurate estimation of evaporation flux needs to take into account the fractionation processes between surface water, atmospheric moisture and the boundary layer forming between them. If the relative humidity is 100% an equilibrium between the liquid and the vapour phase will be established. This equilibrium fractionation depends

only on temperature and has been described above. Craig and Gordon (1965) have developed the principles of the conceptual model of isotopic exchange between surface water and an under saturated atmosphere (relative humidity <100%) for applications in oceanographic studies. They introduced a saturated layer between the liquid water and the turbulent atmosphere. Fractionation during evaporation therefore takes place as a result of (a) equilibrium fractionation between liquid water and the saturated layer of vapour at a given temperature and (b) kinetic fractionation between the saturated layer of vapour and the turbulent atmosphere.

3.3 Stable isotopes in soil

3.3.1 Attenuation

In the unsaturated zone an attenuation of seasonal variations of the isotopic composition of precipitation takes place. This is a result of hydrodynamic dispersion within the soil, where the infiltrating water travels at different velocities through pores with a range of different sizes and in some cases also through cracks, fissures or macropores (see modelling Chapter 5). In fine-grained soils the depth at which the seasonal signal is damped out tends to be less than in coarse soils. In fractured or karstified rocks attenuation is expected to be slow and depth of full attenuation relatively large. The depth at which the isotopic signal becomes stable was found to reach 3 to 5 m in fine-grained soils (Zimmermann, Münnich and Roether, 1967) and up to 9 m in gravel (Eichinger *et al.*, 1984). The isotopic composition of soil water is affected by several processes in the soil: firstly, the original input function is smoothed by dispersion. At the same time selective abstraction of soil water by plants may remove different fractions of infiltrated rainwater during summer and winter and thereby changing the average composition. The example in Figure 3.16 shows that heavy summer rainfall is removed selectively by

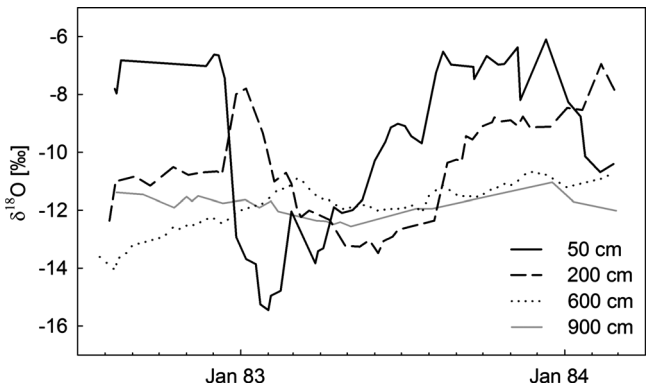

Figure 3.16 Isotopic composition of soil water at different depths in the gravel plain (Munich/Bavaria in Germany), graph redrawn with permission of Eichinger *et al.*, 1984).

plant transpiration. The weighted average of precipitation and percolating water can therefore differ.

The distribution of isotopes in soils can be used for estimating several aspects of soil water movement and vadose zone hydrology. The distribution with soil depth can be evaluated or time series of isotopes at different depths. The approach of Zimmermann *et al.* (1967) can be used as an approximation for saturated soils. For this approach the isotope profile in the soil is treated as an equilibrium state between the upward convection induced by soil evaporation and the downward diffusion of depleted water, resulting in:

$$E = D^* \frac{\ln\left(\frac{\delta}{\delta g}\right)}{z} \tag{3.24}$$

where E represents evaporation, D the liquid diffusivity of isotopes δ the isotope content of liquid water, δ_γ the isotopic composition of at greater depth and z depth, corresponding to a weighted mean of percolating water. This approach is only applicable for soil evaporation directly from the soil surface of a wet soil. It is not applicable for unsaturated zones and does not give information other than that on direct soil evaporation (e.g. total evapotranspiration).

If the percolating water reaches the water table before the seasonal signal has been fully attenuated, these fluctuations will also be found in the groundwater. Depth of attenuation is relevant as it determines whether seasonal fluctuations in the groundwater of the recharge area are to be expected. If seasonal fluctuations are damped out completely, samples can be taken to be representative for the location; otherwise time series sampling needs to be carried out.

If seasonal variations can be identified in the soil profile, the position of seasonal variations can be used to mark water of a specific year or event. The tritium-peak

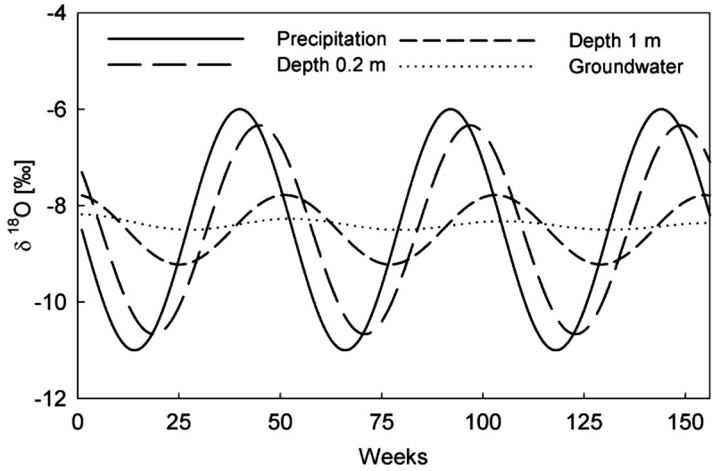

Figure 3.17 $\delta^{18}O$–$\delta^{2}H$ variability at different depths in the soil. With increasing depth the amplitude deceases and the peak shifts.

resulting from thermonuclear bomb tests has been used for this approach. In drylands with low recharge rates and in thick unsaturated zones, this approach can still provide recharge estimates. The recharge rate is defined by:

$$R = \frac{T_{total}}{\sum_{i=1}^{n} w_i * T_{pi} * e^{(-\lambda * t)}} \quad with \quad T_{total} = \int_0^{\infty} T(\varsigma) * \theta(\varsigma) * dz \tag{3.25}$$

where R is the mean annual recharge, w_i a weight transforming precipitation into effective precipitation, T_{pi} the tracer concentration of i years before present, n the years since the time series of the input function starts. T_{total} is calculated by integrating the tracer concentration $T(\zeta)$ at different depths multiplied with the respective soil water content $\theta(\zeta)$ along the whole soil profile. In humid areas and in most cases where the unsaturated zone is thinner, this peak has already passed through the unsaturated zone.

The use of stable isotopes is based on a similar approach. Instead of the tritium peak, the seasonal peaks of summer and winter rainfall are identified. The recharge rate R is then obtained simply by integrating the soil moisture down to an observed peak at the depth z_p and by dividing it by the time since the input into the soil zone $T_{peak.}$

$$R = \frac{\int_0^{z_p} \theta(\varsigma) * dz}{T_{peak}} \tag{3.26}$$

This method is limited by the dispersion of isotopic signals with depth. The attenuation of seasonal variation itself is the basis for another group of methods using stable isotope information in soils.

For a time series of stable isotopes at a given point Maloszewski *et al.* (1983) have developed an approach for relating amplitude attenuation to residence time. The residence time would then be defined by:

$$t = \frac{\sqrt{\left[\frac{A_{precipitation}}{A_{flow}}\right]^2 - 1}}{\omega} \tag{3.27}$$

where ω is the transformed time period and $A_{precipitation}$ and A_{flow} are the respective amplitudes in rainfall (input) and flow (output). This method was developed for groundwater systems and applied to soil water. Stewart and McDonnell (1991) used this approach for soils and derived soil water residence times. Recently this approach was applied by Wenninger (2007).

Lysimeter studies were used by Maloszewski and Zuber (1982), Maciejewski *et al.* (2006) and Maloszewski *et al.* (2006a) to fit combined models of residence time distributions. A combination of an exponential model and a piston-flow model provided a good fit between modelled and measured isotope concentrations and allowed to derive flow velocities and mean residence times (see Section 7.2.2).

3.4 Stable isotopes in surface and groundwater

The isotopic input of precipitation is modified by fractionation processes during recharge. An excellent review of the isotope effects in the transition from rainfall to groundwater for semiarid and arid zones was prepared by Gat (1995). In this chapter an overview of evaporation, attenuation of seasonal variations, biases in the average isotopic composition and of mixing of groundwater is given. The influence of water-rock interactions on the stable isotopes ^{18}O and ^{2}H is only detectable in systems with specific conditions (hydrothermal springs, volcanic volatiles) and will not be dealt with. An introduction is given by Hoefs (1997). Weighted averages of the isotopic composition of precipitation and groundwater may differ and be biased. This happens if selective recharge occurs from precipitation events with a specific isotopic composition (Figure 3.18).

Recharge from flash floods has been observed to cause an isotopic depletion of the groundwater as compared to precipitation under arid conditions. This finding has been interpreted to result from selective activation of runoff and subsequent recharge by very intensive and exceptionally depleted precipitation (Levin, Gat and Issar, 1980). The effect of a bias between the average composition of precipitation and groundwater samples as well as of evaporation is shown below. On a secular time scale, a bias between the *actual* average isotopic composition of rainfall and groundwater may indicate that the groundwater was recharged during a period with a different isotopic signal in the precipitation.

3.4.1 Temporal variability of stable isotopes in runoff

As Frederickson and Criss (1999) have pointed out the isotopic variation of runoff is caused by the isotopic variation of runoff weighed by runoff rates. A simplified approach can be applied from the assumption that the isotopic input function is sinusoidal. Attenuation of the isotope signal and residence times can be determined

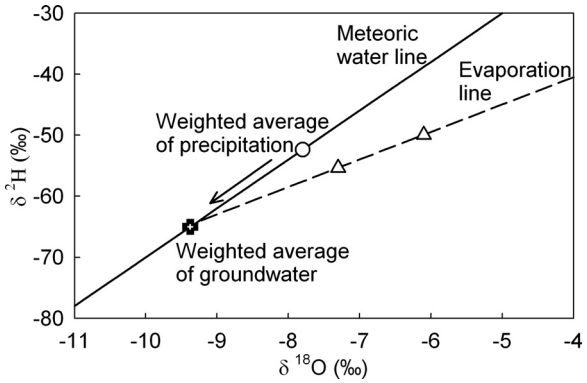

Figure 3.18 Weighted averages in the isotopic composition of precipitation (circle), of groundwater (cross) and partially evaporated surface water (triangles).

using Equation (3.27). Often a deviation from the ideal sinusoidal shape is observed. This bias is mainly caused by a superposition of the source strength of generated runoff and the isotopic signal. A good approximation of observed isotopic variation $\delta^{18}O_{river}$ in runoff can often be obtained by applying a weighing function that accounts for the variability of generated runoff. This weighing function can be approximated by using observed precipitation amounts P_i at time intervals t_i. Equation (3.28) uses a time constant T_C.

$$\delta^{18}O_{river} = \frac{\sum \partial_i P_i \exp(-t_i/T_C)}{\sum P_i \exp(-t_i/T_C)} \tag{3.28}$$

Often T_C of the hydrologic response of the basin and of the isotopic signal is assumed to be equal. In fact, it can differ significantly. A further refinement – at the expense of an additional parameter – can be achieved by identifying individual time constants.

3.4.2 Temporal variability of stable isotopes in groundwater

Before a meaningful interpretation of the spatial distribution of stable isotopes can be made, the temporal variability of stable isotope data must be examined. Information on residence times and flow velocities can be derived from the temporal variability. On the other hand, if the seasonal variation is small or negligible as compared to spatial differences, a regional analysis can be carried out.

Temporal variations in groundwater occur where the isotopic variations in the precipitation are not attenuated in the unsaturated zone and then once more in the saturated zone, in other words where the depth to the groundwater table is smaller than the depth of attenuation. Variations in the isotopic composition of groundwater are most likely where depth to the groundwater table is small, reflecting isotopic variability in rainstorms and recharge.

Figure 3.19 shows the variability of rainfall and the response of a spring with high residence time (above). Springs with smaller residence times exhibit seasonal variations (below). The stability of groundwater values with time can be visualized in time series plots, in bi-plots or frequency distributions of re-sampling campaigns. Also, frequency distributions of deviations between δ^{18}O and δ^{2}H values can be considered in detail. Time series data show the influence of rivers or recharge events and can be used to identify and locate groundwater components with short residence times.

The analysis of temporal variation with time already presented above for soils was developed for aquifer systems. For the time series of stable isotopes at a given point Maloszewski *et al.* (1983) have developed an approach for relating amplitude attenuation to residence time in the case of a sinuosidal input function and an exponential distribution of residence time. The residence time t would then be defined by Equation (3.27).

This method has been used by Pearce, Stewart and Sklash (1986). Equation (3.28) can also be used when estimated recharge is used as a weighting function.

The models presented extensively in Chapter 5 can be used to 'fold' input functions and to produce a resulting time series of isotopes in groundwater.

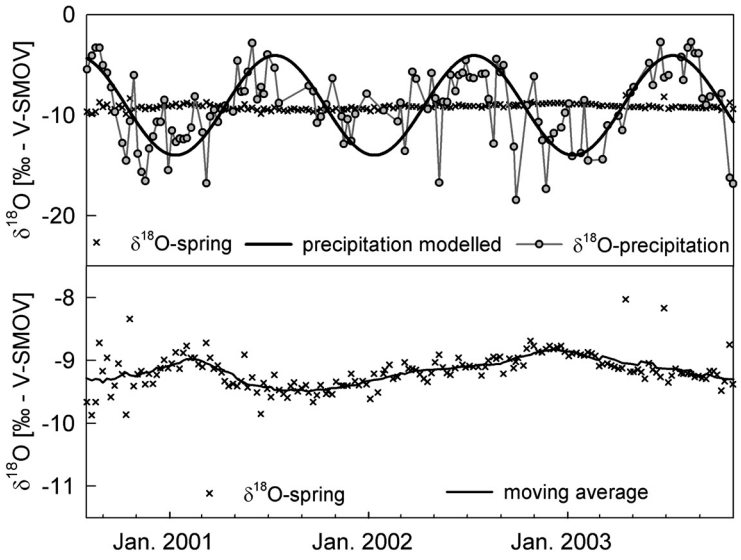

Figure 3.19 Time series of δ^{18}O indicating groundwater and rainfall time series.

The analysis of groundwater systems can also be based on a mass balance approach of water and of stable isotopes. The balance equation writes:

$$\frac{d(V^*\delta_V)}{dt} = \alpha^* P^* \delta_P - Q_{out}{}^* \delta_{Q_{out}} \tag{3.29}$$

where δ_i represent the respective isotopic composition of the hydrological component identified by the subscript I and where α is a weighting factor for effective precipitation.

3.5 The use of environmental isotopes for hydrological system analysis

A regional distribution of $\delta^{18}O$ can be used to identify the source of groundwater, mainly recharge altitude. When using oxygen isotopes it should be checked that evaporation effects do not occur or have been corrected for. In order to facilitate interpretation of data the expected mean $\delta^{18}O$ value of direct recharge at the local altitude can be plotted.

Stable isotopes have also been used to study hydrological systems and to identify flow components. Many applications are based on an end member mixing analysis (EMMA) and inverse modelling (IM) or on the analysis of dispersion of the seasonal variation. The end member mixing analysis is based mainly on measurements of water chemistry and isotopes assuming complete mixing between independent, distinct and conservative tracers. The mixing analysis provides an intrinsic integration of time and space for the examination of areas with scarce hydrologic information. EMMA includes various types of models using environmental tracer data and has been applied for runoff component separation (Sklash and Farvolden, 1979; Buttle, 1994).

Several environmental tracers have been used for end member analysis. In hydrological studies stable isotopes of water have been used (δ^{18}O or δ^{2}H). Further studies have included Silica or for some applications quasi-conservative substances such as Cl^{-}.

The basis equation of EMMA can be derived from the mass balance of water and tracer. If we consider two flow components Q_1 and Q_2, having respective concentrations c_1 and c_2 that mix completely in a flow Q_M with a resulting concentration c_M, it is evident from the conservation of mass of water and mass of tracer that:

$$Q_M = Q_1 + Q_2 \quad \text{and} \tag{3.30}$$

$$c_M Q_M = c_1 Q_1 + c_2 Q_2 \tag{3.31}$$

by rearranging, we get:

$$Q_1 = Q_M * \frac{c_M - c_1}{c_1 - c_2} \quad \text{and} \quad Q_2 = Q_M - Q_1 \tag{3.32}$$

This method is based on some requirements regarding the environmental tracer data. A significant difference between end members must exist, the accuracy of the method is directly linked to the range between c_1 and c_2 divided by the analytical precision. The two end member mixing is based on the assumption that the system is in a steady state, that is that flow and concentrations do not change within the time period and system boundaries are considered. Finally, it is assumed that there are no other flow components contributing to the mass balance of water or tracer.

This approach can be extended to three or more flow components with independent and conservative environmental tracers (Uhlenbrook and Hoeg, 2003). The development of equations is always based on the initial equations of water and tracers. In Figure 3.20 a runoff component analysis is shown based on the end members' rainfall and deep groundwater.

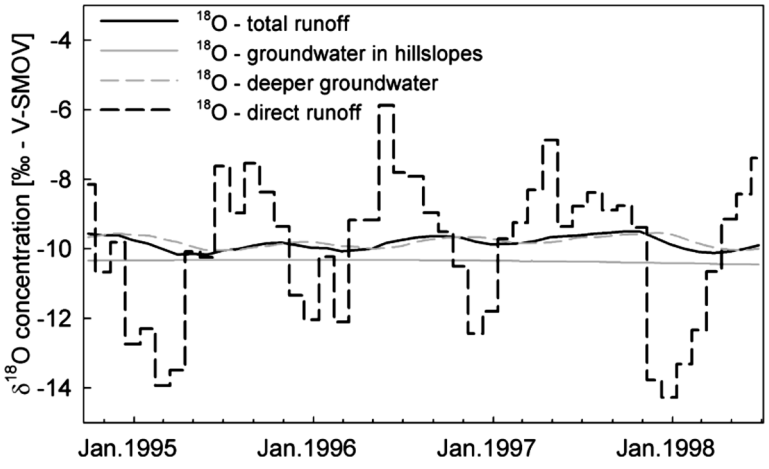

Figure 3.20 Variations of isotope ratios in different compartments of the hydrological system.

3.6 Nitrogen isotopes and origin assignment

Environmental tracers can be used to decipher the origin of solutes and pollutants. The combination with age dating information provides a straightforward approach for developing solutions for management problems. The origin analysis of nitrate shows how the nitrate entered the aquifer system. Stable isotopes of nitrate help to distinguish the possible sources: mineral fertilizers, organic fertilizers (manure) or mineralization of N-bearing substances in the soil and rainfall.

The origin of ammonium and nitrate in groundwater can be investigated by nitrate isotope analysis (Högberg, 1997). While earlier works have relied only on the δ^{15}N-nitrate fingerprint, advanced analytical methods also allow one to determine δ^{18}O-nitrate and to improve the reliability of nitrate origin assignment. The combination of δ^{15}N-nitrate and of δ^{18}O-nitrate is used to determine the isotopic composition of groundwater to that of the potential sources (Durka *et al.*, 1994).

Due to the large oxygen isotopic contrast between nitrates produced in the atmosphere and those produced by microbial processes in the soil (nitrification), the oxygen isotopes in nitrate are particularly useful for the identification of nitrates from fertilizer and atmospheric nitrates. The δ^{18}O of nitrates produced by nitrification varies regionally because one oxygen atom in the nitrate is derived from oxygen gas and two oxygen atoms are derived from soil water or groundwater.

The δ^{15}N-nitrate depends in part on that of the nitrogen source; however, this original signature may be modified by exchange with soil nitrogen and by ammonia volatilization and denitrification. The systematic shift in δ^{15}N-nitrate and δ^{18}O-nitrate

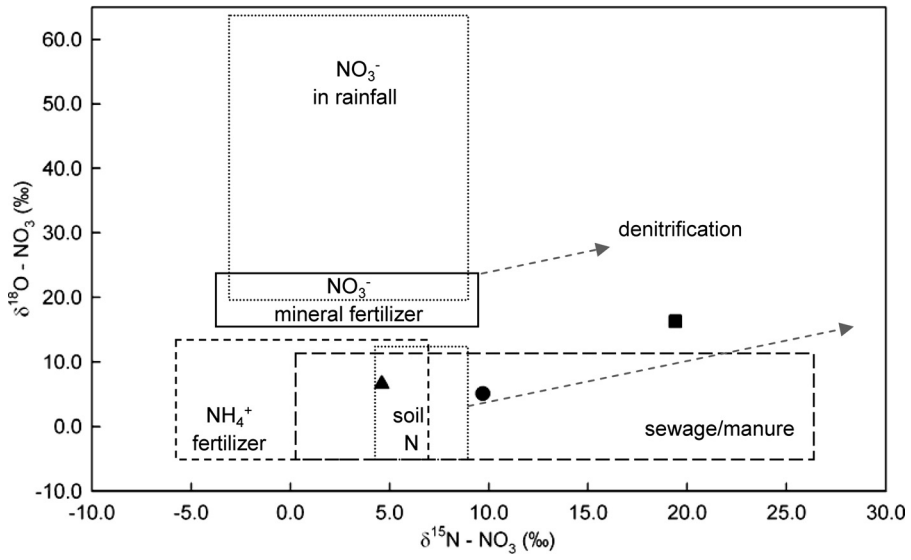

Figure 3.21 Results of nitrate isotope analysis.

allows for identifying denitrification processes that represent a natural remediation. The possible sources of nitrate are:

- nitrate from organic or mineral fertilizers (agriculture),
- ammonium/nitrate from sewage plants or losses from the sewage system,
- ammonium/nitrate from waste dumps.

Ammonium is synthesized technically by Haber-Bosch synthesis from ambient air. As a consequence the isotope ratios correspond to those of air δ^{15}N (-3 to 2‰). Mineral nitrate fertilizer is synthesized from ambient air nitrogen and oxygen. During the synthesis the δ^{15}N increases slightly – this results in δ^{15}N of -1 to 5‰. Most of the oxygen in the nitrate fertilizer stems from ambient air oxygen with a δ^{18}O-nitrate value of about 23‰ V-SMOW. The measured δ^{18}O-nitrate values are in the range of 17 to 22‰. Litter, nitrate stemming from soil nitrification and sewage/manure have similar δ^{18}O-nitrate values close to 0‰ but differ in the δ^{15}N signal.

The process of ammonia evaporation causes an enrichment of heavier nitrogen isotopes and hence increases the δ^{15}N value. Denitrification causes a characteristic increase of both the δ^{15}N and δ^{18}O-nitrate values in the remaining nitrate. Of course these changes of the isotopic composition should correlate with decreasing nitrate concentrations as nitrate is being transformed to nitrogen gas and removed from the system. It is important to check and validate whether the observed changes in the isotopic composition of the remaining nitrate correspond to a decrease of total dissolved nitrate in groundwater. This can be done by plotting δ^{15}N against $1/NO_3$ or $\ln(NO_3)$.

3.7 Age dating

3.7.1 Tritium

The radioactive isotope of hydrogen, ^{3}H (tritium), has a half life of 12.43 years. It decays to ^{3}He by β^- emission. Tritium levels are given as absolute concentrations in tritium units (TU). One tritium unit is defined as one ^{3}H atom per 10^{18} atoms of hydrogen, causing a radioactivity of 0.118 Bq per kg of water. Tritium is measured by liquid scintillation counting of β^- decays. Tritium is produced naturally in the upper atmosphere from nitrogen by neutron impacts of cosmic radiation. It enters the water cycle by precipitation with a seasonal and spatial variation in tritium fallout. Natural fallout is higher in higher geomagnetic latitudes. For northern mid-latitudes a natural level between 3.4 and 6.6 TU has been reconstructed from wines (Kaufmann and Libby, 1954). Thermonuclear bomb tests, starting in 1951, have overdriven this natural level for several decades.

Tritium levels in rainfall have exceeded the naturally occurring levels in the environment by several orders of magnitude. However, the impact of ^{3}H fallout has been

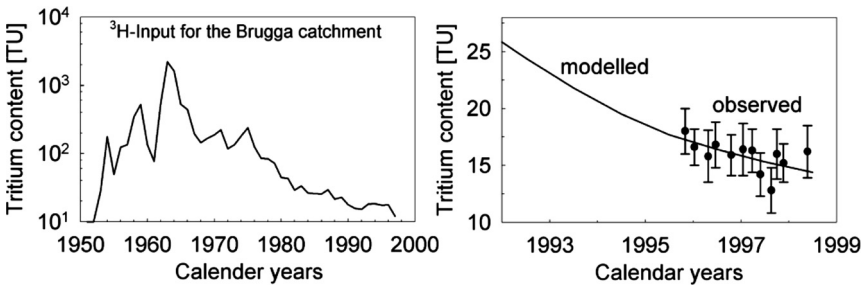

Figure 3.22 Input function for tritium, catchment response observed and modelled.

less pronounced in the southern hemisphere as compared to the northern hemisphere resulting from an asymmetric distribution of tritium emissions from bomb tests and an air mass circulation barrier along the equator. Due to low input levels of tritium in the southern hemisphere, natural attenuation by decay and mixing with pre-bomb groundwater with unique tritium levels can often be used for qualitative interpretation only. Repeated sampling of tritium (Figure 3.22) allows for a modelling of tritium decline and provides a more reliable mean of determining residence times.

Tritum decays to the noble gas ^{3}He. Since the absolute activity of ^{3}H has decreased and almost reached the level of natural input, the combined used of ^{3}H/^{3}He helps to define groundwater ages based on the ratio of both isotopes. The method has been proposed early by Tolstikhin and Kamensky (1969) and used in oceanography and limnology. Weise and Moser (1987), Schlosser *et al.* (1988) and Poreda, Cerling and Solomon (1988) have published applications in shallow aquifers. The application of this method requires adequate sampling techniques that allow one to preserve the concentration of the highly volatile noble gas. The method is based on the equation:

$$T = {}^1\!/\!_\lambda{}^* \ln\left(\frac{{}^3He^*}{{}^3He + 1}\right) \tag{3.33}$$

with T a groundwater age, λ the decay constant for tritium. ^{3}He* must correspond to the tritiogenic concentration, that is derived from the decay of tritium only. Other, atmospheric and geogenic sources of ^{3}He will bias results. The total helium measured in the groundwater sample is composed of dissolved atmospheric helium in equilibrium with the atmospheric partial pressure, excess helium entrapped in recharge water, helium released by emanations from the mantle of the earth and helium released by nuclear tests. The atmospheric dissolved ^{3}He can be determined from neon noble gas measurements. The correction for other sources can be carried out based on the measurement of ^{3}He/^{4}He ratios. Solomon and Cook (2000) suggest:

$$\begin{aligned} {}^3He^* = 4He_m R_o &- R_{sol}[{}^4He_{sol} + (Ne_m - Ne_{sol})\alpha R_{He-Ne}] \\ &- R_{rad}[{}^4He_m - {}^4He_{sol} - (Ne_m - Ne_{sol})R_{He-Ne}] \end{aligned} \tag{3.34}$$

where ^4He_m and Ne_m are the measured concentrations of ^{4}He and Ne, R_o is the measured $^3He/^4He$ ratio, R_{sol} is the $^3He/^4He$ ratio for water that is in isotopic equilibrium with the atmosphere, R_{rad} is the ratio of nucleogenic ^{3}He to radiogenic ^{4}He and $R_{He\text{-}Ne}$ is the Helium/Neon ratio in the atmosphere. The subscript in Ne_{sol} and $^4He_{sol}$ identifies the concentrations that correspond to the equilibrium solubility with the atmosphere, both depend on temperature. The fractionation factor α holds for the air-water isotope fractionation for Helium. This equation can be simplified to:

$$^3He^* \approx 4He_m R_o - R_{sol} \tag{3.35}$$

for samples that do not contain radiogenic ^{4}He and for which excess air can be neglected. The development of the $^3He/^3H$ ratio as an age indicator starts only at the groundwater surface, once the system is closed. In the vadose zone helium is lost by gas diffusion. As Solomon and Cook (2000) point out, the method is less sensitive for older waters and requires precise determinations of excess air. The method also requires a good sampling as air bubble entrapment. Degasing and contamination need to be avoided. The presence of mantle helium close to major fault zones, geothermal fields or geologically young igneous rocks may prohibit the application of this method as the concentration of geogenic sources may exceed the ^{3}He derived from tritium decay by an order of magnitude.

3.7.2 Dating with gases (CFC, SF_6)

Chlorofluorocarbons (CFCs) are synthetic organic compounds and have been developed in the early 1930s. CFCs have marked the global atmospheric system and they have also entered and traced the hydrologic cycle. Data on concentrations of CFCs and Sulfurhexafluorid (SF_6) can be used to trace the flow of young water (less than 50 years) (Busenberg and Plummer, 1993; Oster, Sonntag and Münnich, 1996). CFCs are not inflammable and not toxic. A recent review of their global impact on groundwater containing major references is given in Höhener *et al.* (2003). Several reviews exist on dissolved gases as environmental tracers in subsurface hydrology: Noble Gas Geochemistry (Ozima and Podozek, 1983), Dissolved Gases in Subsurface Hydrology (Solomon, Cook and Sanford 1998), Chemical and Isotopic Groundwater Hydrology (Mazor, 2004). A textbook on CFC application is available (IAEA, 2006).

For dating purposes three main substances are used that are abbreviated as CFC-11, CFC-12 and CFC-113. Their concentrations are measured and compared to the concentration curve of CFCs in rainwater of the last 50 years. In general, the absolute concentrations and the ratios of pairs of CFCs are used.

Chlorofluorocarbons (CFC-11, CFC-12, CFC-113) and sulfur hexafluoride represent an alternative method for dating subsurface water (Katz *et al.*, 1995; Beyerle *et al.*, 1999; Busenberg and Plummer, 2000). Unlike constant concentrations of noble gases, CFCs and SF_6 are released from anthropogenic sources. Air mixing ratios of CFCs show a monotone increase of concentrations through the 1970s and 1980s due to the comparatively high atmospheric lifetimes (approx. 45 years for CFC-11; 87 years for CFC-12;

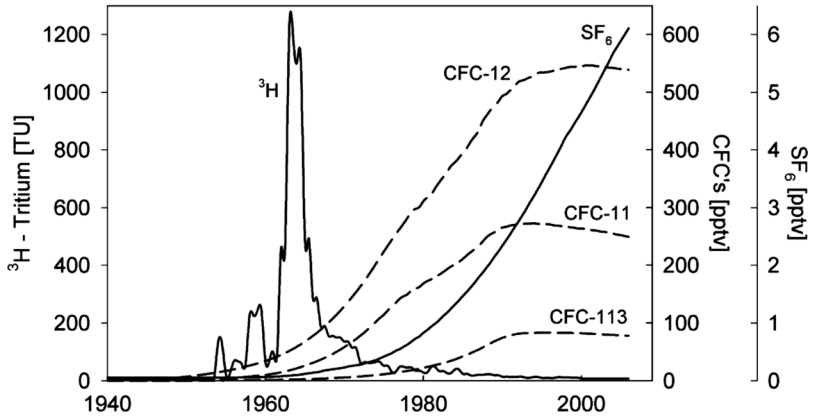

Figure 3.23 Input function for tritium and CFSs. Concentrations are given in parts per trillion volume.

100 years for CFC-113 (Volk *et al.*, 1997)). CFC-11 and CFC-113 peaked in 1993 and 1994, CFC-12 peaked in 1999, as a result of the limit to CFC release in 1987, SF_6 continues to increase. CFCs have been used in oceanic studies since the late 1970s as tracers of oceanic circulation and mixing processes. CFCs have then been introduced as environmental tracers to hydrologic and hydrogeologic studies (Busenberg and Plummer, 1992). Their applicability for very young groundwater (post 1995) is limited because the concentration in the atmosphere has stopped increasing and is actually decreasing.

Their concentration in the atmosphere – the input function – during the last 50 years has been reconstructed (Cunnold *et al.*, 1997). From chemical and physical studies their solubility and the influences of pressure and temperature on the solubility in water are known. Finally, analytical techniques have been developed to detect CFCs with sufficient precision. Dating with CFCs is based on the following principles:

- concentrations of CFCs in the atmosphere have been reconstructed and are known,
- the solubility under defined temperature and pressure conditions are known for specific CFCs,
- hence, the concentration of specific CFCs in rainwater can be calculated,
- rainwater recharging the aquifer carries the equilibrium CFCs concentration as a signal into the groundwater,
- the measurement of CFCs in groundwater is sufficiently precise to resolve the variations of dissolved CFCs in groundwater within the last 50 years.

The use of gases as environmental tracers is based on Henry's law that means on the linear relationship between the partial pressure of a gas and its concentration as a

dissolved constituent of water. If the input function of the gas is known, the age can be derived from known concentrations. However, the validity of the approach is also based on the validity of Henry's law. Temperature and pressure need to be known as they control the dissolution process. This is not as simple as it may seem, because the dissolution may take place under variable conditions. In addition, excess air – air in excess of the concentrations predicted by Henry's law – have been observed. In order to reconstruct the partial pressure of the dissolving gas at the recharge altitude the total pressure p (Pa) is calculated for a given altitude h (m) (IAEA, 2006):

$$\ln p = -h/8300 \tag{3.36}$$

The dissolved concentration c_i (mol/l) of the gas is calculated according to Henry's law as a function of partial pressure p_i (Pa) and of the Henry constant k_{Hi} (mol/l*Pa)

$$c_i = k_{Hi}{}^* p_i \tag{3.37}$$

$$p_i = x_i(p - p_{H_2O}) \tag{3.38}$$

where x_i is the volumetric ratio of gas in air (pptv). A correction for atmospheric moisture p_{H_2O} (Pa) is taken into account. The dissolution constant k_{Hi} depends on temperature and for saline water also on salinity S (‰ mass ratio). The water temperature T (K) can be taken into account (IAEA, 2006) according to:

$$\ln k_H = a_1 + a_2\left(\frac{100}{T}\right) + a_3 \ln\left(\frac{T}{100}\right) + S\left[b_1 + b_2\left(\frac{T}{100}\right) + b_3\left(\frac{T}{100}\right)^2\right] \tag{3.39}$$

Tables for the coefficients a_1, a_2, a_3, b_1 and b_2 are given in IAEA (2006). For the interpretation of data, measured concentrations are first converted to molar fractions per volume. These molar fractions c_i are used to calculate the initial gas concentration that can be compared to a known input function:

$$x_i = \frac{c_i}{k_H(p - p_{H_2O})} \tag{3.40}$$

The reconstructed concentration at recharge can exceed even present concentrations as a result of several factors. Excess air can be introduced into the groundwater system as a result of nonequilibrium conditions. It is assumed that air bubbles are transferred into the groundwater system by rapid rises of groundwater levels or by air entrapment in the soil or the aquifer. The air bubble may dissolve partially or completely if exposed to hydrostatic pressure. Excess air corrections can be taken into account based on quantitative gas analysis or on noble gas analysis (USGS, 2008; Aeschbach-Hertig *et al.*, 2000; Plummer and Busenberg, 2000; Bauer, Fulda and Schäfer, 2001).

In Figure 3.24 a typical analysis for CFCs is given. The input functions are given as volumetric ratios. Concentrations of CFCs in groundwater are measured with gas chromatography with electron capture detector (GC-ECD) and range from picomol/l (pmol/l) to femtomol/l (fmol/l). Based on Equations (3.36)–(3.40) these are converted to original volumetric ratios in the atmosphere and compared to the input functions.

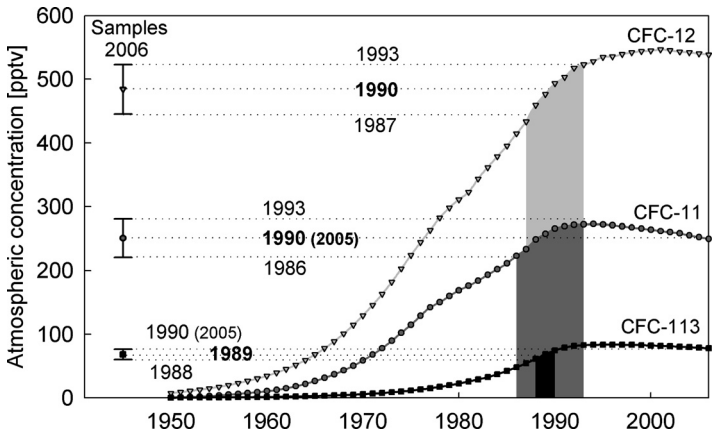

Figure 3.24 Input function of different CFCs (CFC-11, CFC-12, CFC-113) and measured concentrations.

The example below shows a good match of all three measured CFCs. Error ranges are given from ±2–4 years. In the case of CFC-11 and CFC-113 the result is not unique, two different recharge years are possible.

Bi-plots reduce the uncertainty and confirm whether CFC data are consistent. If the sample is located on the curve being defined by the pair of concentrations, residence times are concordant (Figure 3.25).

All of the graphs above are based on a piston flow model. Often it is useful to calculate the concentration resulting from an exponential model (see Chapter 5). This is done in Figure 3.26 (dashed line).

With only one exception (alluvium) samples are located on the line defined by the exponential model. This indicates that boreholes are located in a phreatic aquifer that is recharged on its entire length.

Local anomalies from the global atmospheric input function might exist at present or might have existed in the past (Oster, Sonntag and Münnich, 1996). In the northern hemisphere especially and close to highly industrialized areas such local effects have

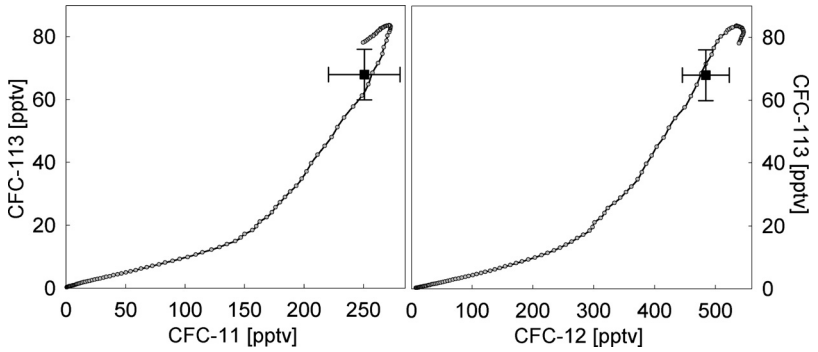

Figure 3.25 Bi-plot of concentrations of CFC-113 and CFC-11 (left) and of CFC-12 and CFC-113.

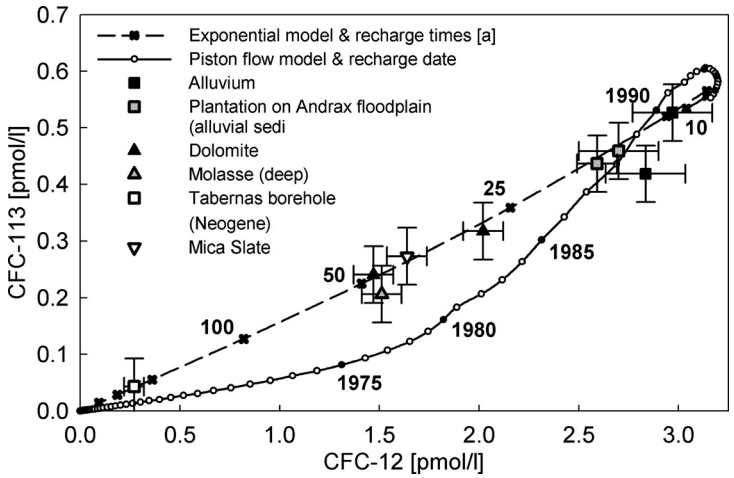

Figure 3.26 Concentrations of CFC-12 and CFC-113 in groundwater corresponding to original atmospheric concentrations for a piston-flow-model (continuous line) and for an exponential model (dashed).

been observed. Measurements of atmospheric samples can help to identify the local anomaly and apply corrections to the global atmospheric input function. In such cases at least a relative order of mean residence times can be established. In other cases local groundwater sources of CFCs exist. Uncontrolled municipal waste dumps (containing refrigerators) may release CFCs locally. In such cases dating with CFCs is often not feasible. The accuracy of the determined age depends on how conservative the transport of CFCs in water actually is. Especially, excess air, the influence of the soil atmosphere and degassing processes may affect the accuracy of CFC dating. Even if one or some of these limitations apply in a certain case, the presence of CFC is a marker for post 1950 influence. CFCs should be used after reconnaissance studies, based on hydrogeologic knowledge of the site conditions and together with other dating tools.

In recent years the role of SF_6 as a trace atmospheric gas has been recognized, mainly for dating post-1990s groundwater (Bauer, Fulda and Schäfer, 2001). SF_6 is produced since the 1960s, primarily as isolation in high voltage elements and as a cleaning agent, but also for shock (noise) absorption in windows. Unlike CFCs, atmospheric concentrations of SF_6 are expected to rise. Currently, the concentration of SF_6 is growing at a global scale because more substance is produced than the environment can destroy, absorb or store. The atmospheric lifetime of SF_6 is estimated to be at least 500 to 1000 years.

SF_6 is analysed with gas chromatography (ECD) (Oster, Sonntag and Münnich, 1996). Concentrations of down to 10^{-16} can be measured. SF_6 is a virtually conservative tracer with small known interactions and physical or chemical decay rates. CFCs enter the water cycle by dissolution in precipitation. Solution is controlled by known equilibria, temperature and pressure dependencies. Excess air, soil gas equilibria and degasing may affect the dating precision. It needs to be considered that SF_6 may also occur naturally in igneous rocks and in volcanic or igneous fluids. Also, the ratio of SF_6 to CFCs can be used as a dating tool.

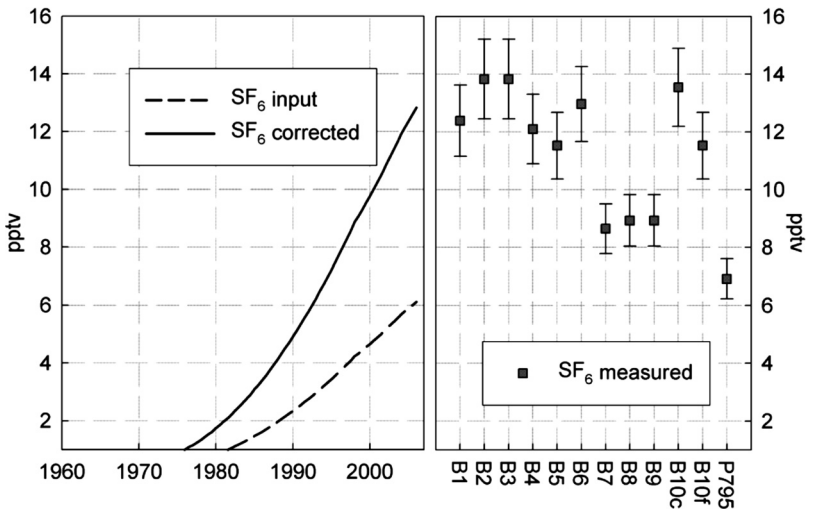

Figure 3.27 Application of gas dating with SF_6.

3.7.2.1 Dating with other noble gases

Other gases have also been used for groundwater age dating. The application of ^{39}Argon (Loosli and Oeschger, 1968; Loosli, 1983; Loosli, Lehman and Balderer, 1989; Forster, 1983; Forster, Moser, Loosli, 1984) can fill the gap between tracers with short half-lives and ^{14}C. ^{85}Krypton is an alternative for CFCs, SF_6 and tritium dating. It has a half-life of 12.5 years and atmospheric concentrations are increasing continuously. Dating of groundwater with ^{85}Krypton has been developed by Salvamoser (1981) and a series of applications exist (Smethie *et al.*, 1992; Loosli, 1989; Cook and Solomon, 1997; Bauer, Fulda and Schäfer, 2001). Krypton in groundwater needs to be enriched from about 6000 l in order to get sufficient accuracy for age dating. Enrichment is carried out in situ with a spray and strap method (see IAEA, 2006; USGS, 2008).

An interesting aspect of ^{85}Kr is the possibility to combine it with other tracers that have a significantly different input function. The ^{85}Kr-tritium harp combines both tracers and allows determining the residence time and the mixing with an old component (see Figure 3.28). The 'harp' is constructed by folding the input function with an exponential model (see Chapter 5). A dispersion or a piston-flow model or any combination of these can be used as well. The resulting line is the mixed with a 0.0 component – a component containing no tritium and Krypton-85. Data plotted into this diagram indicated the residence time (intersection with the 100% line) and the amount in % of tracer-free groundwater as well.

3.7.2.2 ^{14}C-dating

Radiocarbon is produced in the upper atmosphere through cosmic radiation. Collision of a neutron with nitrogen produces ^{14}C and a proton. ^{14}C enters the troposphere as

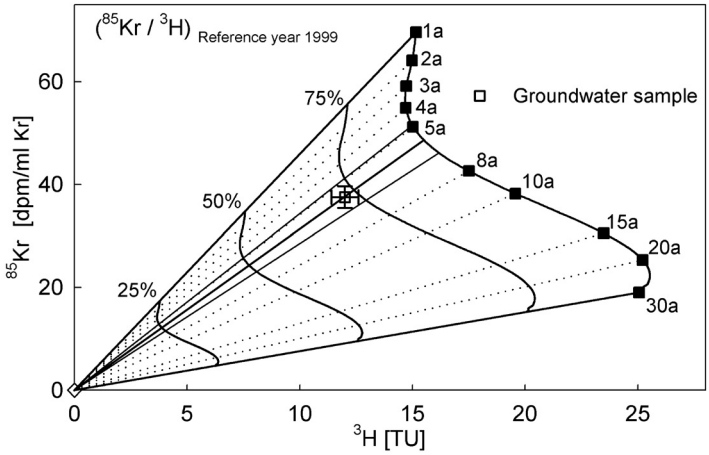

Figure 3.28 Krypton-85 and tritium harp.

CO_2 and participates in the hydrologic and biologic carbon cycles. It is radioactive and decays according to:

$$a_t = c^* a_0{}^* e^{-\lambda^* t} \qquad \Rightarrow \qquad t = -\frac{1}{\lambda}{}^* \ln\left(\frac{a_t}{c^* a_0}\right) \tag{3.41}$$

where $\lambda = 1.2097\text{e-}4$ is the decay constant, c is a dilution factor, a_t is the ^{14}C activity at time t and a_0 the initial ^{14}C activity (Geyh and Schleicher, 1990). The half-life of ^{14}C is 5730 years. Activities are expressed as *p*ercent of the standard '*modern carbon*' abbreviated as '*pmC*'. The standard is defined as 95% of the ^{14}C activity in 1950 of a NBS oxalic acid standard. It corresponds to the activity of wood grown in 1890 before the combustion of fossil carbon. The actual ^{14}C in the sample is measured by scintillation counting or with accelerator mass spectrometry. In some hydrogeological systems where groundwater is isolated from input of modern carbon sources containing ^{14}C, radioactive decay of ^{14}C in dissolved inorganic and organic carbon compounds may be used for dating. Time t since groundwater became isolated from the atmosphere and the soil can be derived from the ratio of actual and initial activities a_0 and a_t according to Equation (3.41).

Some difficulties arise for the estimation of the initial activity a_0. The activity in living plants is about 100% pmC. However, the production of ^{14}C in the upper atmosphere fluctuates with time. Calibration with oak tree dendrochronology (Stuiver and Kra, 1986; Stuiver and Reimer, 1993) and corals (Bard *et al.*, 1990) showed that initial ^{14}C activity varied by about 10% during the Holocene. In addition anthropogenic effects have altered the natural regime. Combustion of fossil fuel has diluted the atmosphere with ^{14}C-free CO_2. Nuclear weapons testing and power plants have released artificial ^{14}C into the atmosphere.

An additional '*reservoir effect*' needs to be taken into account for the application of ^{14}C to groundwater systems (Geyh, 1995). Soil water equilibrates with soil CO_2 during infiltration. $HCO_3{}^-$ concentrations increase and solution of available primary or secondary carbonates ensues (Münnich, 1968). The solution of ^{14}C-free carbon

Table 3.1 Dilution factors for a preliminary estimation of initial ^{14}C activities at the groundwater surface for different environments (Vogel, 1970)

Dilution factors	Recharge environment
0.65–0.75	For karst systems
0.75–0.90	For sediment with fine grained carbonate
0.90–1.00	For crystalline rocks

reduces the initial activity of carbon compounds in deep percolation. Several correction methods have been proposed. Vogel (1970) derived initial activities using statistical analysis of measured activities in the recharge area. For different recharge environments the following average factors provided in Table 3.1 were suggested.

The $^{13}C/^{12}C$ ratio has been proposed as a parameter for correcting ^{14}C initial activities (Pearson, 1965). Ratios of the stable carbon isotopes ^{13}C and ^{12}C are compared to the VPDB standard (*V*ienna *P*ee *D*ee *B*elemnitella) and given in δ-notation. The correction method takes advantage of the large difference between $\delta^{13}C$ values of soil CO_2 and of marine limestone. C_3 plants reach $\sim -23‰$ VPDB, C_4 plant values range from ~ -10 to $-16‰$ (Vogel, 1993). Marine limestone is often close to zero. The correction is calculated with Equation (3.38):

$$c_{\text{Carbon}-13} = \frac{\delta^{13}C_{\text{DIC}} - \delta^{13}C_{carbonate}}{\delta^{13}C_{soil} - \delta^{13}C_{carbonate}} \tag{3.42}$$

where $c_{\text{Carbon}-13}$ is the dilution factor, $\delta^{13}C_{DIC}$ is the measured value in the dissolved inorganic carbon of groundwater, $\delta^{13}C_{carbonate}$ is that of the carbonate which is being dissolved and $\delta^{13}C_{soil}$ stands for the $\delta^{13}C$ value of the soil. Equation (3.42) holds only for closed system dissolution.

The chemical mass balance correction (CMB) is based on the ratio c_{CMB} between ^{14}C-active dissolved inorganic carbon ($m\text{DIC}_{recharge}$) from soil CO_2 and the total carbonate content at the time of sampling ($m\text{DIC}_{final}$). Different means of estimating $m\text{DIC}_{recharge}$ and $m\text{DIC}_{final}$ exist. The initial carbonate content during recharge can be estimated by assuming pH and pCO_2 and calculating the equilibrium concentrations of different carbonate species. The final carbonate content can either be measured (titrated) or calculated from chemical data as listed in Equation (3.43).

$$c_{\text{CMB}} = \frac{m\text{DIC}_{recharge}}{m\text{DIC}_{final}} \quad with$$

$$m\,DIC_{final} = m\text{DIC}_{recharge} + mCa^{2+} + mMg^{2+} - mSO_4^{2-} + \frac{1}{2}\left(mNa^{+} + mK^{+} - mCl^{-}\right) \tag{3.43}$$

Finally the general hydrochemical correction by Fontes and Garnier (1979) is mentioned. This model combines measured $\delta^{13}C$ and major ion concentrations and also accounts for open system dissolution. This approch has not been used due to uncertain estimates of the strongly pH dependent enrichment factor $\varepsilon^{13}C_{CO_2 \leftrightarrow CaCO_3}$ that is required for this model.

Box 3.1

Example for age dating with two groundwater samples that were taken in a semiarid basin in southern Spain (Andarax catchment). The aquifers from which samples were taken are porous aquifers. One aquifer consists of alluvial sediments of about 20–30 m thickness, the second aquifer consists of tertiary alluvial and colluvial sediments.

The samples were taken from active production boreholes. Sampling was carried out after about 10 borehole volumes were pumped and in situ parameters were stable. Sample water was filled into an imerged glass bottle contained in a gas-tight container. Analysis of samples was made with GC-ECD.

The laboratory report gives a concentration of dissolved gas in water as a concentration in picomol (pmol/l) or femtomol per litre (fmol/l). There are two ways of analysing data. The most common method consists of calculating the initial atmospheric volume ratio in pptv (=parts per trillion volume) from the concentration of the dissolved gas in water. The ambient temperature during dissolution of the gas and the atmospheric pressure need to be known for the application of Henry's law. The atmospheric pressure is derived from the international barometric formulae based on the elevation. The reconstructed initial atmospheric pressure that was needed to produce the measured dissolved concentration at defined conditions of temperature and pressure is compared to the input function in pptv. The match indicates when recharge took place. In case of input functions that are not monotonous more than one recharge year can be obtained. This method has advantages as it allows one to compare values taken at different recharge conditions more easily.

The second method consists of calculating the concentrations that would result in groundwater for specific recharge temperature and a specific elevation or pressure. Then the laboratory values of dissolved trace gases in water are compared to the input function (as dissolved gas in water). This method has advantages if different water types are mixed with specific models (exponential model, dispersion model). Because mixing of groundwater containing specific concentrations of dissolved gases that might have been recharged at different altitudes (and not of air masses) takes place the second approach should be applied if we intend to use dissolved concentrations for mixing or transport models. If dissolved concentrations of trace gases are to be compared in the same graph they need to be normalized to a standard elevation and standard temperature (e.g. 200 m and 8 °C). Then this allows the graphical presentation of different samples as dissolved concentrations in water in one graph as shown in the Figure Box 3.1 below. Both approaches are shown in this box.

The Calculation of Dissolved Input Concentration in Groundwater

The Henry coefficient (k_H) for CFC-12 and CFC-113 for a given temperature and salinity is calculated using Equation (3.26) with a recharge temperature of

(*continued*)

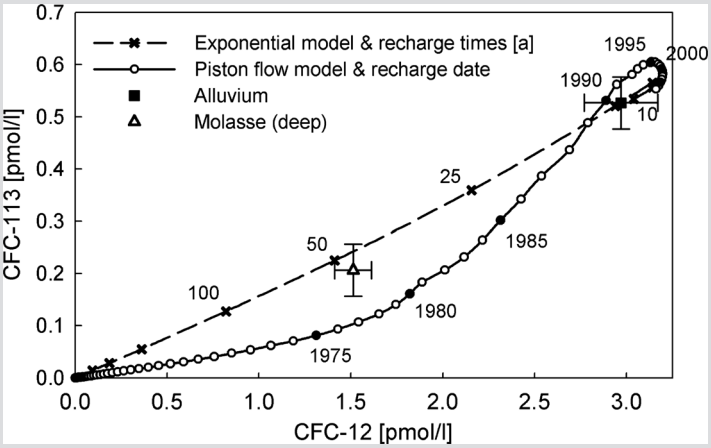

Box Figure 3.1 Bi-plots for concentrations of CFC-12 and CFC-113 for a piston flow and for an exponential model.

8 °C (281.15 K), a salinity of 5 per mil (corresponds to the samples) and parameters a_i and b_i taken from IAEA (2006). For CFC-12 we get:

$$\ln k_H = -124.44 + 185.43\left(\frac{100}{281.15}\right) + 51.638\ln\left(\frac{281.15}{100}\right) + 5\left[-0.149 + 0.095\left(\frac{281.15}{100}\right) - 0.016\left(\frac{281.15}{100}\right)^2\right]$$

$$= -5.1457 \Rightarrow k_H = 0.00576$$

and for CFC-113:

$$\ln k_H = -136.129 + 206.475\left(\frac{100}{288.15}\right) + 55.896\ln\left(\frac{288.15}{100}\right) + 5\left[-0.028 + 0.006\left(\frac{288.15}{100}\right) + 0\left(\frac{288.15}{100}\right)^2\right]$$

$$= -4.962 \Rightarrow k_H = 0.007$$

The partial pressure is calculated according to Equations (3.23) and (3.25) for a recharge altitude of 200 m.a.s.l. as:

$$\ln(p) = \left(\frac{-200}{8300}\right) = -0.0241 \Rightarrow p = 0.976Pa$$

$$p_i = xi(t)(0.976)$$

We can then use the atmospheric input function of atmospheric concentrations and calculate the corresponding concentration in groundwater using x_i and $\ln k_H$. For CFC-12 and CFC-113 (data taken from http://cdiac.ornl.gov/oceans/new_atmCFC.html). Table Box 3.1 lists some of these values that represent the piston flow model respectively exponential mixing for different residence times (see Equation 5.81.2, Chapter 5) listed in Table Box 3.2 .

Box Table 3.1 Yearly values – Piston flow assumption

Year	2005	2000	1995	1990	1985	1980	1975	1970	1965
CFC-12 [mol/l]	3.185	3.19	3.129	2.888	2.314	1.812	1.311	0.757	0.397
CFC-113 [mol/l]	0.566	0.591	0.603	0.531	0.301	0.161	0.081	0.041	0.02

Box Table 3.2 Exponential mixing

Residence time [a]	2	5	10	25	50	100	250	1000
CFC-12 [mol/l]	3.043	2.997	2.702	1.860	1.173	0.667	0.290	0.149
CFC-113 [mol/l]	0.623	0.590	0.484	0.288	0.168	0.091	0.038	0.019

The Calculation of Dissolved Concentrations in Groundwater for Standard Conditions

Sample no. 1 is taken at an altitude of 200 m.a.s.l. in the alluvium of the channel. The annual temperature averages 15 °C. Measurements result in a CFC-12 concentration of 2.2 pmol/l and CFC-113 concentration of 0.39 pmol/l. Sample no. 2 is taken at an altitude of 495 m.a.s.l. in the molasse. The CFC-12 concentration is 0.39 pmol/l and the CFC-113 concentration is 0.15 pmol/l. Here the average temperature is about 14.5 °C.

The concentrations are converted to a standard height of 200 m.a.s.l. and a temperature of 8 °C as follows. For CFC-12:

$$c_1(200m, 8^\circ C) = (1 + (15 - 8)^*0.05)^*2.2^* \exp\left(\frac{200 - 200}{8000}\right) = 2.97 pmol/L$$

$$c_2(200m, 8^\circ C) = (1 + (14.5 - 8)^*0.05)^*1.1^* \exp\left(\frac{495 - 200}{8000}\right) = 1.51 pmol/L$$

And for CFC-113:

$$c_1(200m, 8^\circ C) = (1 + (15 - 8)^*0.05)^*0.39^* \exp\left(\frac{200 - 200}{8000}\right) = 0.53 pmol/L$$

$$c_2(200m, 8^\circ C) = (1 + (14.5 - 8)^*0.05)^*0.15^* \exp\left(\frac{495 - 200}{8000}\right) = 0.21 pmol/L$$

(*continued*)

By comparison of theses values and the calculated theoretical values it is possible to estimate a residence time and respectively a mean age of the groundwater. The upper curve represents values corresponding to an exponential model. The lower full line represents concentrations of dissolved gas in groundwater corresponding to a piston-flow model.

In this case the sample taken in the alluvium has a short residence time. It is not possible to distinguish whether it corresponds to a piston-flow or to an exponential distribution. In the case of piston-flow the samples were recharged in 1990 (15 years before sampling), in case of an exponential distribution the residence time is slightly above 10 years. The second sample plots close to the line derived for an exponential distribution. The corresponding mean residence time is about 50 years. The same concentration can also result from a binary mixing of various different end members.